A quantitative assessment of the behavior of metallic elements in urban soils exposed to industrial dusts near Dunkerque (Northern France)

Marine Casetta[1], Sylvie Philippe[1], Lucie Courcot[1], David Dumoulin[2], Gabriel Billon[2], François Baudin[3], Françoise Henry[1], Michaël Hermoso[1], Jacinthe Caillaud[1]

[1] LOG, Laboratoire d'Océanologie et de Géosciences, Université du Littoral Côte d'Opale, Université de Lille, CNRS, IRD, UMR 8187, Wimereux, France

[2] Univ. Lille, CNRS, UMR 8516 – LASIRE, Laboratoire Avancé de Spectroscopie pour les Interactions, la Réactivité et l'Environnement, F-59000 Lille, France

[3] Sorbonne Université – CNRS, UMR 7193 ISTeP – Institut des Sciences de la Terre de Paris, 75005 Paris, France

Correspondence to: Marine Casetta (marine.casetta@univ-littoral.fr)

Abstract

In urban and industrialized areas, soil contamination and degradation caused by industrial dust deposition may pose significant health and environmental risks. Generally, the mobility and thus bioavailability of Potentially Toxic Elements (PTE) are key factors in these issues. In the Dunkerque agglomeration, one of the most industrialized regions in France, the soils are periodically exposed to metallurgical dust fallout, rich in PTE. However, no study has reported the behavior of these PTE once integrated into the soils. The aim of this study is therefore to assess the fate of PTE in the urban soils of Dunkerque in terms of vertical migration and potential bioavailability.

Four soil short cores were collected in the city of Gravelines (Dunkerque agglomeration) along a gradient from industrial emitters to deposition sites. Each soil core was cut into discrete 1-cm-sections for PTE concentration analyses (ICP-AES/MS). Single HCl extractions were performed to evaluate PTE mobility in soils and their behavior according to the current soil parameters. For this purpose, key soil properties were identified, including grain-size distribution, mineralogy, pH, CEC, TOC, calcium carbonates and water contents in addition to the soil chemical composition (XRF, ICP-AES/MS).

The studied soils revealed globally low absorbent capacities for pollutants (CEC averaging 5.3 meq/100g), partially counterbalanced by the buffering effect of calcium carbonates (contents ranging from 8 % to 30 %). Near the industrial emitters, minor (1 < EF < 3) to moderately severe (5 < EF < 10) Enrichment Factors (EF) were highlighted for industrial PTE (Cr, Ni, Mo, Mn, Cd, Zn), in the top 3 cm of soils near the industrial emitters. The contamination profiles of these soils are assigned to atmospheric inputs of metallurgical dust. Using a relatively strong leaching reagent (HCl 1M), we estimated a low

vertical mobility for Cr, Ni and Mo (average leached ratios <25 %) in soils, suggesting their association with refractory phases (natural or anthropogenic). In contrast, Mn, Cd and Zn, related to industrial and/or urban sources, present a higher mobility (average leached ratios > 60 % for Mn and Cd, and about 44 % for Zn).

Our study points out the stability of industrial PTE in soils under the current physicochemical conditions (calcareous soils with a slightly basic pH of 7.8). In this context, the monitoring of industrial PTE in these urban soils is highly recommended, considering (1) the presence of allotment gardens in the vicinity of emitters and (2) the potential evolution of soil conditions due to increasing flood events.

1 Introduction

Soils are essential to the survival of civilizations and terrestrial ecosystems, although they are extremely vulnerable and nonrenewable at the scale of human life (Minami, 2009; Smith et al., 2015; Stavi et al., 2016). The Food and Agriculture Organization of the United Nations recently recorded 5 670 million hectares of land worldwide in declining biophysical conditions (FAO and UNEP, 2021). This report indicates that human activities are responsible for more than 29 % of this deterioration through changes in land uses, soil over-exploitation, climate change, introduction of invasive exotic species or release of pollutants (Emadodin and Bork, 2012; Tetteh, 2015; Dror et al., 2022).

Among the various soil pollutants, Potentially Toxic Elements (PTE) are particularly studied because of the threat that they represent for the ecosystems and human health. This is especially the case when they are mobilized and transferred to groundwater or the food chain (Zhuang et al., 2009; Rajmohan et al., 2014; Sun et al., 2018). Soils act as key interfaces between several environmental compartments, and their physicochemical properties make them both vectors and reservoirs for contaminants (Girard, 2005; Kandpal et al., 2005; Palansooriya et al., 2020; Sarkar et al., 2021). In urban areas, anthropogenic activities significantly contribute to soil pollution by PTE, especially metallurgical activities and mostly via atmospheric deposits (Duzgoren-Aydin et al., 2006; Khademi et al., 2019; Manta et al., 2002). The resulting soil degradation by PTE inputs may cause major health and environmental problems, particularly in areas of increasing density of population (Schulin et al., 2007; Douay et al., 2013; Ortega Montoya et al., 2021).

In the Dunkerque agglomeration (Northern France), over 150 plants facilities constitute a major risk for the environment. In 2021, the local metallurgical industries emitted more than 2 700 t of total dust into the atmosphere, pinpointing concerns about the contamination of the surrounding soils (Registre des émissions polluantes, 2023). To date, only one study has focused on the soils of this area, investigating the spatial distribution of PTE in surficial soils in the city of Gravelines (Dunkerque agglomeration) (Casetta et al., 2024). This study provided critical insights, highlighting (1) an appreciable portion of coals, iron ores, slags and other metallurgical products (> 88 %) in the industrial dust falling in the streets of the city during NE wind and dry periods, (2) a diffuse contamination of soils by PTE associated to industrial dust, such as Cr, Ni, Mo particularly but also Zn, Cd, Mn, and (3) the punctual degradation of the soil quality by industrial dust.

While this previous work revealed the contamination of surface soils by industrial dust, two main questions remain. They relate to the vertical distribution of the metallic contaminants in the soil profiles, and to the capacity of these soils to retain pollutants. These points are crucial, as understanding the behavior of industrial PTE is essential to evaluate their long-term environmental impact, including their potential transfer to groundwater and uptake by biota. The present study is the first to investigate the vertical distribution and possible leaching of PTE (Cr, Mn, Ni, Cu, Zn, Mo, Cd) associated with industrial dust or anthropogenic inputs in selected urban soils (Gravelines). To evaluate the mobility of PTE, single HCl extractions were carried out on four soil short core (0-11 cm). In addition, their physicochemical profiles were established, including grain size distribution, water contents, pH, CEC, calcium carbonates, Total Organic Carbon, major oxide concentrations and mineralogical composition. Using these parameters aims to better understand the interactions between PTE and the soil matrix. Finally, this work seeks to highlight the specific behavior of PTE in soils and their potential link with industrial sources.

2 Material & methods

2.1 Study area and sampling

The city of Gravelines (50°59' N, 2°08' E) is located in Northern France on the North Sea coast (Fig. 1); It has a surface area of 22.66 km^2 and its population was 11 014 in 2019 (INSEE). The climate is temperate: average annual rainfall of 727 mm and annual temperature ranging between 2°C and 22°C (MERRA-2 meteorological data, 1980-2016). The land uses distribution is 52 % of urbanized/industrialized spaces, 22 % of agricultural, 16 % of natural spaces and 10 % of infrastructures. Three metallurgical production sites and one plant for receiving, handling and storing ores in open air were installed less than five km from the city center as result of the construction of the seaport of Dunkerque (industrialized seaport in Fig. 1). The soils of the studied zone were developed on Holocene marine and alluvial clay and sandy sediments, deposited during the Gallo-roman Medieval period and belonging to the Flanders coastal plain (Leplat et al., 1988). In this plain, the soils mainly consist of clayey-sandy materials and are rich in calcium carbonates (median value: 13 %) (Sterckeman et al., 2004). According to the pedological classification of the French Association for Soils Study (AFES), the soils of Gravelines can be ascribed to "Thalassosols", characteristic of a pedogenetic evolution on marine or alluvial deposits (Baize and Girard, 2009; GIS Sol and RMT Sols et Territoires, 2019). In the World Reference Base for Soil Resources (WRB) system (FAO, 2014), they can be classified as Solonchaks, reflecting their development in coastal environments. In this highly populated studied area, the coastal plain is drained through a dense network of channels to avoid flooding from the sea, or by brackish/freshwater. Thus, the characteristics of the studied soils may locally significantly differ from the general type proposed (i.e. solonchaks).

Four sampling stations were selected in the city of Gravelines (Fig. 1) according to: (1) the concentrations in PTE associated to industrial dust fallout (Casetta et al., 2024); (2) the nature of the soil matrices; and (3) their distance to the emission sources. They present 2 types of uses: collective use as parks and green spaces in the city center (station 1), and mesophilic grassland or deciduous planting trees located near the industrial emitters (stations 2, 3 and 4). Short cores of soils under herbaceous cover were collected at the four stations in July 2021 during the summer season using a manual auger and PVC tubes. For each site, one core (diameter of 4.5 cm and depth of 11 cm, in order to sample the upper A horizon) was taken and cut into 1 cm sections using a Teflon core cutting table. Thus, a total of 44 soil samples were analyzed.

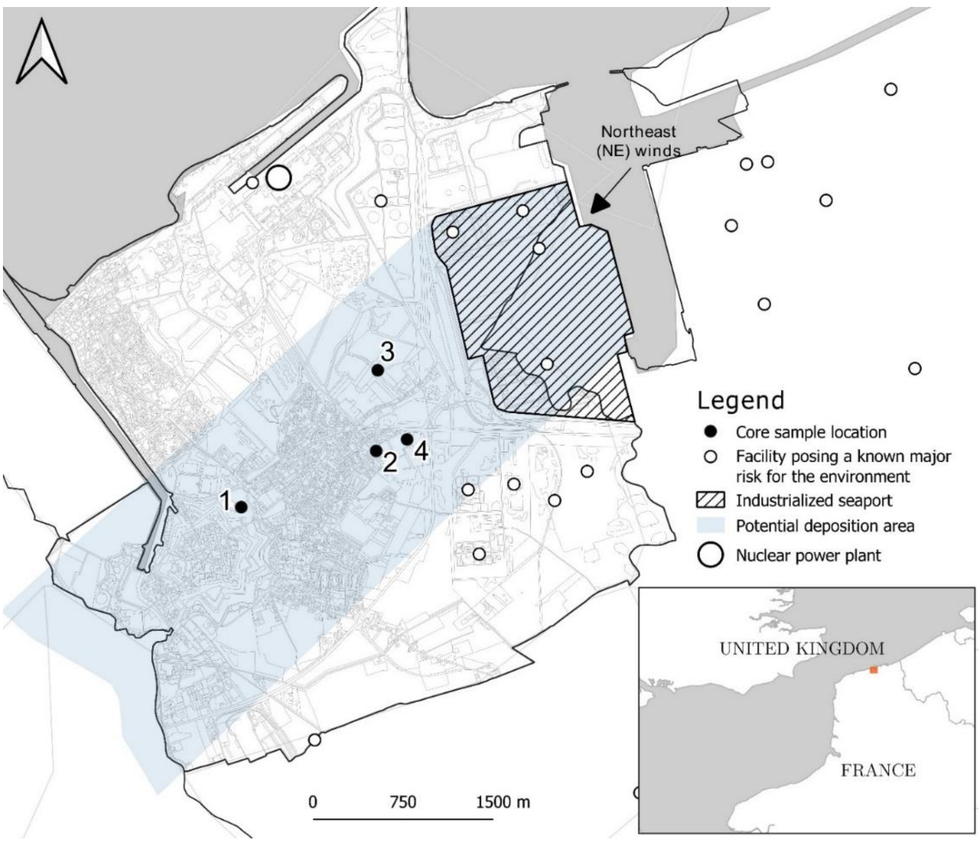

Figure 1: Map of the city of Gravelines indicating the sampling stations located southwest of the industrialized seaport (IGN – BD TOPO® Nord 2023).

2.2 Nature of the soil matrices

2.2.1 General soil parameters

The water content of the soils was determined by weighing samples, before and after drying a 30-g-aliquot at 65°C in a ventilated oven (according to the normative protocol NF EN 1097-5). A combined glass electrode and a pH-Meter were used to measure soil pH in deionized water (1:5 soil: solution) (NF ISO 10390, see Goix et al., 2015). The soil cation exchange capacity (CEC) was determined using a spectrophotometric method based on cobaltihexamine chloride absorbance (Aran et al., 2008). Aliquots of 2 g of dry samples were mixed to a 0.01 N solution of cobaltihexamine chloride during 1 hour. The solution was filtered through 0.22 µm filters (cellulose acetate) after 10 minutes centrifugation (4000 g). The CEC was obtained by measuring the absorbance at 472 nm of the collected mixture.

The grain-size distribution and calcium carbonate contents were measured on the subsurface (0-1 cm), the middle (4-5 cm) and in a deeper layer (9-10 cm) for the four sampled cores. The grain-size distribution was determined on wet samples by laser diffraction. The Coulter LS 13 320 instrument (gallium arsenide, 750 nm wavelength, Brea, USA) measured a particle diameter ranging from 0.375 to 2000 µm. Prior to analysis, organic matter was removed by adding 50 mL of H_2O_2 (35 %), according to the Belgian standard NBN 589-207 §3 (Leifeld and Kögel-Knabner, 2001; Amar et al., 2021). A 2 mm mesh sieve was used to remove the higher size fraction and each soil sample was sonicated to achieved disaggregation. Particle size classes were assigned according to the Soil Science Division Staff (2017) grain-size scale, i.e. 0.375–2.0 µm for the clay fraction, 2.0–20 µm for the fine silt fraction, 20–50 µm for the coarse silt fraction and 50–2000 µm for the sand fraction. A manual calcimeter (OFITTE, Houston, USA; dried and grinded samples) was calibrated with pure calcium carbonate to obtain the total carbonate content ($CaCO_3$) of the soil samples. This content was estimated by the gas pressure emitted after reaction of 1 g of fine powdered sample when adding 20 mL of HCl 20 %. Measurement uncertainties were estimated from three analytical replicates performed on the highest and lowest values during laboratory phases. The absolute uncertainties for the studied soil parameters are as follows: pH ± 0.1; CEC ± 0.2 meq/100 g; $CaCO_3$ content ± 1 %; particle size distribution: clay ± 0.5 %; fine silt ± 2 %; coarse silt ± 2 %; sand ± 3 %.

2.2.2 Total Organic Carbon (TOC) content and characterization by Rock-Eval measurements

The soil samples were analyzed with a Rock-Eval 6 (RE6) Turbo device (Vinci Technologies, Nanterre, France) using the basic setup for soil organic matter analysis (Disnar et al., 2003; Hetényi and Nyilas, 2014). The RE6 technique required two steps: (1) the pyrolysis of 60 mg of finely ground soil (< 250 µm) in an N_2 atmosphere (from 200°C to 650°C; heating rate of 30°C min^{-1}); followed by (2) the oxidation of the pyrolysis residues in an oxygenated atmosphere (from 300°C to 850°C; heating rate of 20°C min^{-1}). Volatile hydrocarbon (HC) effluents during pyrolysis were detected and quantified using Flame Ionization Detection (FID), while oxygen compounds (CO, CO_2) were quantified during the two steps by infrared detection. Measurements resulted in the production of five thermograms (S1 to S5) per sample, corresponding to free hydrocarbons (S1), pyrolyzable hydrocarbons (S2), CO_2 and CO (S3) generated during pyrolysis step, and to CO and CO_2 (S4 for organic residual carbon and S5 for mineral carbon) produced during the oxidation step. The complete description of the method is available in Lafargue et al. (1998) and Cécillon et al. (2018). Finally, the analysis of the different thermograms allowed the calculation of several parameters (Espitalié et al., 1977, 1985; Vandenbroucke and Largeau, 2007), as:

- The Total Organic Carbon content (TOC; wt %) corresponding to the sum of residual and pyrolyzed organic carbon;

- The Hydrogen Index (HI; mg HC/g TOC) corresponding to the quantity of HC released relative to TOC (S2/TOC);
- The Oxygen Index (OI_{RE6}; mg O_2/g TOC) corresponding to the quantity of oxygen released as CO and CO_2 during pyrolysis and relative to TOC and calculated as follows (Lafargue et al., 1998):

$$OI_{RE6} = \left[\left(\frac{16}{28} \times OI_{CO}\right) + \left(\frac{32}{44}\right) \times OI_{CO2}\right]$$

with $OI_{CO} = 100 \times S3_{CO}/TOC$ and $OI_{CO2} = 100 \times S3_{CO2}/TOC$

HI and OI_{RE6} are used to highlight the main type of organic matter present in the studied soils. For this purpose, these index are compared to the Van Krevelen diagram (H/C vs. O/C) of Espitalié et al. (1977).

2.2.3 Major oxide measurement

An energy dispersive X-ray fluorescence spectrometer (Bruker S2 PUMA ED-XRF) was used to measure the concentration of 7 major oxides (Na_2O, MgO, Al_2O_3, SiO_2, K_2O, CaO, Fe_2O_3) on fused soil beads. The spectrometer was equipped with a 50 kV Ag anode tube (maximum power: 50 W; maximum high voltage: 50 kV; maximum current: 2 mA; cooling medium: air) and a high-resolution Silicon Drift Detector (< 141 eV for Mn-Kα1). Spectral data were analyzed by Spectra Elements software version 2.0. Soil samples were dried, sieved (2 mm), ground, homogenized and calcined at 1050°C (loss on ignition: LOI). Then, fused bead specimens were formed by mixing 500 to 1 000 mg of calcinated powder with a lithium tetraborate (33 %), lithium metaborate (67 %) and lithium bromide (< 1 %) mixture. These flux mixtures were loaded in a Katanax® K1 Prime fluxer and heated up to 1060 °C during 20 minutes. Analytical quality of the XRF measurements was controlled by analyzing 11 certified samples of stream sediments. Determination limits (DL) and measurement uncertainties are available in Table S1 in the supplementary materials.

2.2.4 Mineralogy

Mineralogy X-ray diffraction (XRD) studies were carried out using an AXS D4 Endeavor Diffraction System (Bruker; 35 kV, 30 mA; Cu K_α radiations) coupled to a PSD LynxEye detector. Crushed soil samples were examined as random total powder to obtain the total mineralogical composition between 3 and 60°2θ. Background stripping, diffraction peak indexing, mineral identification by comparison with the files of the Joint Committee on Powder Diffraction Standards (JCPDS) and semi-quantitative analysis were carried out using the X'Pert data HighScore software. Thus, a list of four minerals (Table S2 in the supplementary materials) was chosen according to: (1) the best match between the positions of peaks (score); and (2) the quality of the reference based on a calibration with titanium (Reference Intensity Ratio, RIR). For the clay preparation, 0.2 M hydrochloric acid was used to decalcify the soil samples and the excess acid was removed by repeated centrifugations after rinsing with deionized water. Settling was used to isolate the clay-sized fraction (< 2 µm) which was next oriented on glass slides (oriented mounts). Clay minerals are identified between 2.5 and 32°2θ according to the position of the (001) series of basal reflections on air-dried, glycolated (after saturation for 12h in ethylene glycol) and 490°C-heated (for 2 hours) diffractograms (Holtzapffel, 1985). Their semi-quantification was carried out on the glycerol curve using MacDiff software. The reproducibility of technical works and measurements was tested and the relative error was < 5 % (Bout-Roumazeilles et al., 1999).

2.3 Vertical evolution of PTE concentrations

2.3.1 PTE concentrations in total and leached soil samples

An amount of 200 mg of each ground soil samples were digested using first a concentrated HF–HNO_3 mixture (67:33 v:v) and then 2 successive concentrated HCl–HNO_3 mixture (67:33 v:v). Each digestion step lasted 48 hours at 125°C before evaporation. Dissolved samples were finally diluted in 9 mL with acidified ultrapure MilliQ® (Millipore 18.2 MΩ.cm resistivity) water. Each solution was filtered on 0.22 µm filters (cellulose acetate) to remove potential residues. All the reagents were of the optimal/suprapur grade. Single extractions were performed on the same ground soil samples by mixing 1 g of powder with 20 mL of cold 1M HCl for 24 h (Billon, 2001; Philippe et al., 2008). Next, leached samples were centrifuged and the supernatant was filtered on 0.22 µm filters (cellulose acetate) for ICP analyses. This leaching approach using 1M HCl was chosen to match with the high calcium carbonate contents of the studied soils (12 to 30 %), relatively young and developed on Holocene coastal sediments (deposed during the Gallo-roman Medieval period). Indeed, weaker acid concentrations (0.2 M to 0.5 M) and shorter contact time (Madrid et al., 2007; Kubová et al., 2008; Pelfrêne et al., 2020) could underestimate PTE mobility in the leaching solution due to buffering effects of carbonates (Birch, 2017). The 1M HCl extractions is thus supposed to leach, from the soils, metals potentially mobilized through local changes of pH: exchangeable metals, metals weakly bound to organic substances (Waterlot et al., 2017; Pelfrêne et al., 2020), metals precipitated with calcium carbonates or associated with amorphous or poorly crystallized Fe-Mn-oxides or hydroxides (Yong et al., 1992; Rao et al., 2010). According to Hamdoun et al. (2015) and Yu et al. (2021), this technique allows the estimation of the general mobility and reactivity of PTE in the soil matrices. The total content of the studied PTE was determined both in total and leaching solutions using ICP-AES (Agilent 5110 VDV, for Cu) and ICP-MS (Agilent 7850, for Cr, Mn, Ni, Zn, Mo and Cd). The accuracy and precision were controlled using two sediment standard reference materials (MESS-3 and PACS-2), twelve analytical triplicates and six blank samples. The recovery values of the reference standards and the detection limits are available in Table S3 in the supplementary materials. To discuss the PTE mobility in soils, Table 1 summarizes their environmental characteristics (uses, environmental sources and pathways, mobility in relation to environmental conditions). Considering these data, it is expected in the studied soils a high mobility for Cu, Mn, Mo, Ni, Zn and in a lesser extent Cd, and a low mobility for Cr after HCl 1M leaching.

Table 1: Environmental geochemistry of the studied PTE (after Goldberg et al., 1996; Baize, 1997; Reimann and De Caritat, 1998; Crea et al., 2013)

Element	Environmental sources and pathways	Mobility in soils			
		Acidic cond.	alkaline cond.	oxidizing cond.	reducing cond.
Cr	Steel works (stainless steel, alloys, chrome plating), electrometallurgy, combustion of natural gas, oil and coal, agriculture (some P-fertilizers)	very low	very low	very low	very low
Mn	Steel production, mining and smelting, traffic (antiknock agent in gasoline), agriculture (fertilizers, fungicides), rock weathering, windblown dust	high	very low	very low	high
Ni	Steel works (alloys, electroplating), petroleum refining, catalysis, traffic, fuel/coal combustion, agriculture (fertilizers)	high	very low	medium	medium
Cu	Cu-mining and smelting, other non-ferrous smelters, electrical industry, plastic industry, steel works (alloys), sewage sludge, agriculture (pesticides, manure), geogenic dust, rock weathering	very high	very low	medium	very low
Zn	Zn smelters, galvanizing, alloys, combustion, traffic, waste water, roof, agriculture (pesticides, manure), geogenic dust	high	very low	high	very low
Mo	U mining, Mo mining and smelting, alloys, oil refining, oil and coal combustion, sewage sludge, phosphate detergents, agriculture (P fertilizers), geogenic dust, weathering	high	very high	high	very low
Cd	Coal combustion, iron and steel mills, electroplating, Pb smelting, incinerators, traffic, sewage sludge, agriculture (fertilizers)	relatively high	medium	variable	very low

2.3.2 PTE Enrichment Factors (EF)

Trace metal concentrations were compared to those of agricultural ploughed soils of the French Flemish Coastal plain (the so-called Wateringues marine plain), supposed to be preserved from potential contamination sources (because distant from industrial activities, busy roads, houses) (Sterckeman et al., 2004). The EF evaluates the degree of metallic contamination of soils by distinguishing anthropogenic from natural metal concentrations (Ye et al., 2011; Harb et al., 2015). Aluminium (Al) is commonly used as a normalizing element (Brady, 1984; Duodu et al., 2017). In this sense, EF were calculated following Eq. (1):

$$EF = (C_n/C_{Al})/(B_n/B_{Al}) \quad (1)$$

where C_n and C_{Al} are the concentration of a metal element n and the concentration of Al in the sample, respectively; B_n and B_{Al} are the concentration of a metal element n and the concentration of Al in the Wateringues marine plain background (median values of the agricultural soils from (Sterckeman et al., 2004)), respectively.

2.4 Data analysis

Maps were made using QGIS 3.10 (QGIS Development Team, 2023). Statistical computing and graphics were performed on R software (R Core Team, 2022) using the following packages: FactoMineR (Lê et al., 2008), ggplot 2 (Wickham, 2016), corTest (Yu et al., 2020), factoextra (Kassambara and Mundt, 2020) and corrplot (Wei and Simko, 2021). As suggested by Chapman (1996), all concentration values below the detection limit (DL) were replaced by half of the DL for the statistical analyses. As the collected data present a non-parametric distribution, the correlations between results were highlighted using the Spearman's correlation test (R).

3 Results

3.1 Soil cores properties

3.1.1 Physicochemical parameters

The physicochemical properties of the soil cores are available in Table 2. The study of soil parameters reveals significant variations between the four sampled stations and along depth profiles. Soil pH from all sampled stations is slightly basic (range: 7.4 – 8.3; average value: 7.8). Notable heterogeneity in soil textures is highlighted between cores. Core 1 presents a "sandy loam" texture with the highest sand contents (40 % to 58 %) and the lowest clay contents (9 % to 12 %). Conversely, cores 3 and 4 are characterized by a "silt loam" texture, higher clay contents (13 % to 19 %) and lower sand values (8 % to 26 %). Core 2 presents an intermediate "loam" texture with clay and sand values ranging from 12 % to 16 % and from 31 % to 41 %, respectively (Richer-De-Forges et al., 2008). No important vertical variation is observed in the grain-size distribution of soil cores, except in core 4 in which clay content increases in subsurface in an inverse proportion to sand content.

Table 2: Physicochemical characteristics of the sampled cores. SD: standard deviation and "-" means no data. TOC: Total Organic Carbon; CEC: Cationic Exchange Capacity; LOI: Loss On Ignition at 1050°C. Detection Limits are available in table S1. Station 1: park and green spaces; Stations 2, 3 and 4: mesophilic grassland or deciduous planting trees.

Core	Depth (cm)	pH	Water content (%)	TOC (%)	CEC (meq /100 g)	$CaCO_3$ (%)	Clay (%)	Fine silt (%)	Coarse silt (%)	Sand (%)	LOI (%)	Na_2O (%)	MgO (%)	Al_2O_3 (%)	SiO_2 (%)	K_2O (%)	CaO (%)	Fe_2O_3 (%)
	0-1	-	28	2.6	4.6	8	11	29	7	54	9	0.5	< 0.7	< 1.9	83	1.2	4.0	1.1
	1-2	-	31	3.1	5.1	-	-	-	-	-	11	< 0.5	< 0.7	< 1.9	81	1.2	4.0	1.1
	2-3	7.8	32	3.4	5.4	-	-	-	-	-	11	0.6	< 0.7	< 1.9	80	1.1	4.5	1.1
1	3-4	-	32	3.5	5.5	-	-	-	-	-	11	0.5	< 0.7	< 1.9	81	1.1	4.2	1.1
	4-5	7.7	31	3.1	5.8	8	12	37	12	40	10	< 0.5	< 0.7	< 1.9	82	1.2	4.0	1.1
	5-6	-	29	2.9	5.6	-	-	-	-	-	10	0.7	< 0.7	< 1.9	81	1.1	4.0	1.1
	7-8	-	25	2.5	5.2	-	-	-	-	-	9	0.6	< 0.7	< 1.9	83	1.2	4.2	1.1

Core	Depth (cm)	pH	Water content (%)	TOC (%)	CEC (meq /100 g)	$CaCO_3$ (%)	Clay (%)	Fine silt (%)	Coarse silt (%)	Sand (%)	LOI (%)	Na_2O (%)	MgO (%)	Al_2O_3 (%)	SiO_2 (%)	K_2O (%)	CaO (%)	Fe_2O_3 (%)
	9-10	7.7	24	2.3	5.7	9	9	27	6	58	9	< 0.5	< 0.7	< 1.9	82	1.3	4.5	1.2
	10-11	-	23	-	5.0	-	-	-	-	-	9	0.7	< 0.7	< 1.9	82	1.4	4.6	1.1
	Average	7.7	28	2.9	5.3	8	11	31	8	51	10	0.6	< 0.7	< 1.9	82	1.2	4.2	1.1
	SD	0.04	4	0.4	0.4	1	1	5	3	10	1	0.1	-	-	1	0.1	0.3	0.0
	0-1	7.4	29	2.5	4.8	11	16	41	12	31	11	0.6	< 0.7	2.2	76	1.3	6.4	1.9
	1-2	-	29	2.4	5.0	-	-	-	-	-	11	< 0.5	< 0.7	2.6	77	1.3	6.4	1.8
	2-3	-	28	2.2	4.8	-	-	-	-	-	10	< 0.5	< 0.7	2.6	76	1.5	6.7	1.9
	3-4	-	22	1.6	4.4	-	-	-	-	-	10	< 0.5	< 0.7	2.9	77	1.3	6.7	1.9
2	4-5	7.8	20	1.3	3.8	12	17	34	12	38	9	< 0.5	< 0.7	2.8	78	1.2	6.7	1.9
	5-6	-	18	1.1	3.8	-	-	-	-	-	9	< 0.5	< 0.7	2.3	78	1.5	6.8	2.0
	7-8	-	18	1.0	3.6	-	-	-	-	-	9	< 0.5	< 0.7	2.9	74	1.2	6.7	1.9
	9-10	8.0	17	1.0	3.7	12	12	33	14	41	8	-	-	-	-	-	-	-
	10-11	-	16	-	3.5	-	-	-	-	-	8	0.5	< 0.7	2.4	79	1.3	6.9	2.0
	Average	7.7	22	1.7	4.2	12	15	36	13	36	9	0.6	< 0.7	2.6	77	1.3	6.7	1.9
	SD	0.3	5	0.7	0.6	1	2	5	2	5	1	0.1	-	0.3	2	0.1	0.2	0.0
	0-1	-	57	4.7	7.3	25	14	41	20	26	23	< 0.5	< 0.7	4.2	53	1.4	14.8	2.6
	1-2	7.5	49	4.1	7.2	-	-	-	-	-	21	< 0.5	< 0.7	4.5	57	1.4	16.8	2.8
	2-3	-	45	3.2	6.7	-	-	-	-	-	20	0.6	< 0.7	4.7	54	1.5	15.7	2.6
	3-4	-	40	2.7	6.2	-	-	-	-	-	19	0.6	< 0.7	4.1	55	1.4	16.1	2.7
3	4-5	8.0	35	2.1	5.8	28	15	38	22	25	19	< 0.5	< 0.7	4.5	56	1.4	16.4	2.8
	5-6	-	31	1.7	5.4	-	-	-	-	-	18	0.5	< 0.7	4.2	54	1.5	16.4	2.7
	7-8	-	28	1.2	5.0	-	-	-	-	-	17	0.8	< 0.7	4.8	56	1.5	16.6	2.8
	9-10	8.0	26	1.1	4.8	30	16	42	18	24	17	0.5	< 0.7	5.6	56	1.4	16.8	2.7
	10-11	-	26	-	4.7	-	-	-	-	-	16	< 0.5	< 0.7	4.4	54	1.5	15.2	2.7
	Average	7.8	37	2.6	5.9	28	15	41	20	25	19	0.6	< 0.7	4.5	55	1.4	16.1	2.7
	SD	0.3	11	1.3	1.0	3	1	2	2	1	2	0.1	-	0.5	1	0.1	0.7	0.1
	0-1	-	46	3.3	6.8	15	19	54	19	8	15	< 0.5	< 0.7	4.2	66	1.4	9.6	2.6
	1-2	7.8	43	3.1	6.7	-	-	-	-	-	15	< 0.5	< 0.7	4.0	67	1.4	9.5	2.6
	2-3	-	40	2.7	6.5	-	-	-	-	-	14	0.6	< 0.7	4.1	66	1.3	9.6	2.6
	3-4	-	36	2.2	6.2	-	-	-	-	-	13	0.6	< 0.7	4.1	67	1.4	9.6	2.7
4	4-5	7.8	31	1.6	5.7	15	16	48	23	13	13	0.5	< 0.7	4.2	68	1.6	10.2	2.7
	5-6	-	23	1.3	5.6	-	-	-	-	-	12	0.7	< 0.7	2.9	75	1.3	6.4	1.6
	7-8	-	22	1.1	5.3	-	-	-	-	-	12	< 0.5	< 0.7	4.7	69	1.4	10.2	2.7
	9-10	8.3	19	1.0	5.2	15	13	41	24	24	12	0.6	< 0.7	4.5	68	1.6	10.3	2.7
	10-11	-	19	-	5.2	-	-	-	-	-	11	0.5	< 0.7	4.7	68	1.6	10.1	2.8
	Average	8.0	31	2.0	5.9	15	16	48	22	15	13	0.6	< 0.7	4.2	68	1.5	9.5	2.6
	SD	0.30	11	0.9	0.7	0	3	7	3	8	2	0.1	-	0.5	3	0.1	1.2	0.3
	Total average	7.8	30	2.3	5.3	16	14	39	15	32	13	0.6	-	3.8	70	1.4	9.2	2.1
	SD	0.2	10	1.0	1.0	8	3	8	6	15	4	0.1	-	0.9	11	0.1	4.6	0.7

The CEC values range from 3.5 to 7.3 meq/100 g and are globally low, according to Rengasamy and Churchman (1999). Maxima CEC values are measured in the subsurface of cores 3 and 4 [0-1cm] (7.3 and 6.8 meq/100 g, respectively) while minimum CEC is measured in core 2 [10-11cm] (3.5 meq/100 g). $CaCO_3$ contents present no significant variation with depth but are higher in core 3 (average: 28 %) and 4 (average: 15 %). The lowest $CaCO_3$ values are observed in core 1 (average: 8 %). The average water content by core can be sorted as follows: core 3 (37 %) > core 4 (31 %) > core 1 (28 %) > core 2 (22

%). While it presents homogeneous vertical profiles in cores 1 and 2, the water content significantly decreases with depth in cores 3 (57 % to 26 %) and 4 (46 % to 19 %). SiO_2, CaO and Fe_2O_3 contents appear stable with depth but present significant variations between cores. The highest SiO_2 contents are observed in cores 1 and 2 (> 78 %). The lowest are notable in core 3 (57 %) where Al_2O_3 and CaO concentrations follow an inverse pattern (Al_2O_3 > 4.2 % and CaO > 15.2 %). Fe_2O_3 contents globally range from 1.9 % and 3.0 % except on core 1 (average: 1.1 %).

TOC content shows little variation between cores (average value: 2 %; standard deviation: 1 %) and globally decreases with depth. The highest value is measured in the subsurface of core 3 (4.7 %). Core 1 presents another pattern and remains relatively stable along the profile (from 2.3 to 3.5 %). The OI and HI records (Table S4 in the supplementary materials) present slight differences between the subsurface and the deepest layer of soil cores 2, 3 and 4 (HI values ranging from 152 to 335 mg HC/g TOC; OI_{RE6} values ranging from 154 to 218 mg O_2/g TOC). Cores 3 and 4 follow a relatively close trend with intermediate values of HI and higher values of OI_{RE6}. Core 1 exhibits a similar pattern to core 2 for OI_{RE6} but has the highest HI values. The calculation of hydrogen (HI) and oxygen (OI_{RE6}) indexes (Table S4) allows the approximation of the bulk chemistry of the soil organic matter (Espitalié et al., 1977; Vandenbroucke and Largeau, 2007; Saenger et al., 2013). As each biological component (proteins, lignins, lipids, humic and fulvic acids…) is characterized by a particular location within the Van Krevelen diagram (H/C vs O/C ratios) (Preston and Schmidt, 2006; Balaria et al., 2009; Falsone et al., 2012), the position of the studied samples in the pseudo Van Krevelen diagram (HI : OI_{RE6}) indicates their approximate bulk chemistry. Although HI and OI_{RE6} values present slight heterogeneity, the distribution of points on the pseudo Van Krevelen diagram reveals that the organic carbon detected in the four soil cores globally occurred as fulvic acids (Fig. 2) (Saenger et al., 2013).

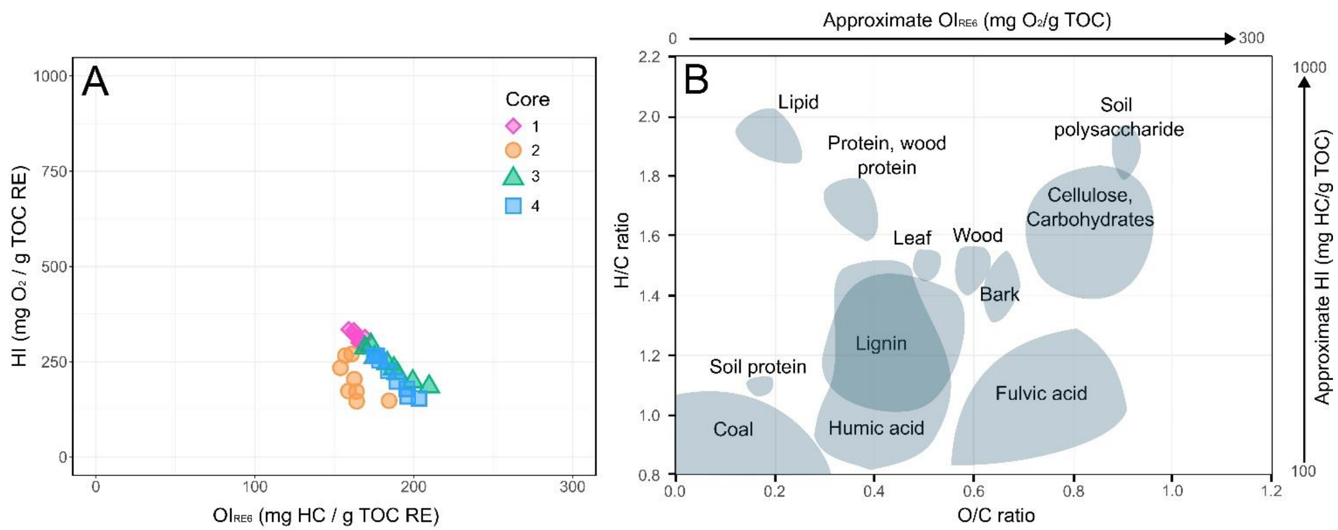

Figure 2: (A) Position of soil samples in the pseudo Van Krevelen diagram (HI vs. OI_{RE6}) according to the different soil cores. (B) location of soil molecules and biological compounds in the Van Krevelen diagram (H/C vs. O/C) and approximate correspondence in the pseudo Van Krevelen (Preston and Schmidt, 2006; Balaria et al., 2009; Falsone et al., 2012).

3.1.2 Total and clayey mineralogical composition

Figure 3 presents the vertical profile of total and clayey mineralogical composition in the four soil cores (the complete data set is available in Table S5 in the supplementary materials). The study of total minerals indicates a dominance of quartz (> 50 %) in all cores and no significant evolution of their composition downcore. Core 1 is characterized the highest quartz values (> 70 %) and the lowest feldspars, calcite and micas concentrations, with average concentrations of 3 %, 4 % and 9 %, respectively. Core 3 has a different behavior with the highest calcite and micas concentrations (22 % and 20 %) and lowest quartz and felspars values (54 % and 5 %). A predominance of quartz is also observed on cores 2 and 4 (range: 67 % to 81 %). The same proportions of calcite, micas and feldspars are measured in these two cores (averaging 10 %, 12 % and 4 %, respectively). The clay minerals nature differed from core 1 to core 4 with an increasing percentage of smectite and a decreasing percentage of all the others (illite, kaolinite, chlorite). While illite dominates the assemblage of the clay minerals in cores 1 and 2 (> 41 %), smectite is the preponderant clay mineral in cores 3 and 4 (> 50 %). All the soil cores present higher smectite percentages with increasing depth (range: 34 % to 67 %) and higher illite (32 % to 56 %), kaolinite (14 % to 22 %) and chlorite (9 % to 15 %) percentages in the subsurface (< 3 cm).

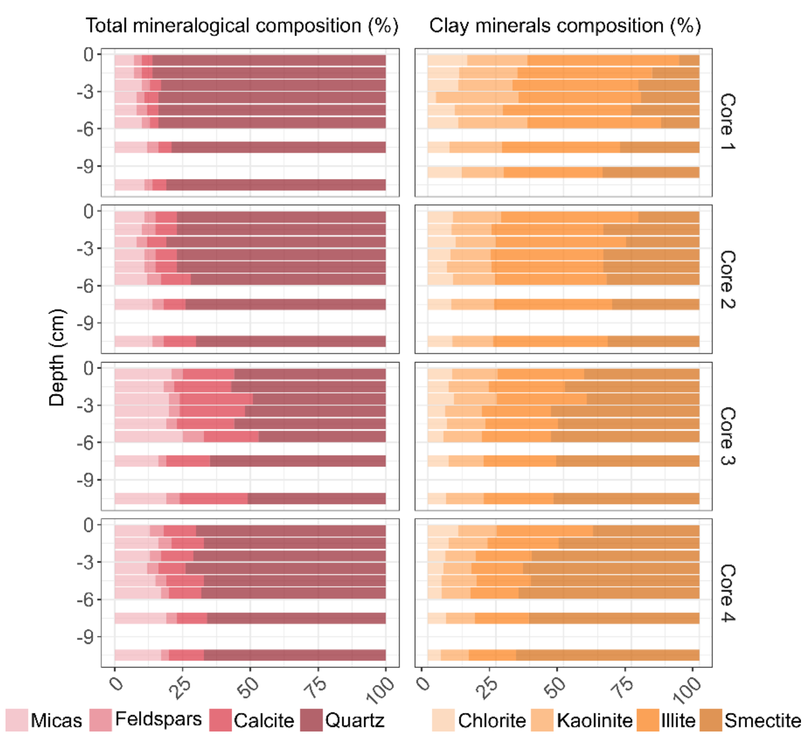

Figure 3: Vertical profiles of total (left) and clay (right) minerals on the four studied cores.

The physicochemical parameters of soils (Table 2) support the AFES pedological classification of the upper soils of Gravelines as “Thalassossols”: the samples exhibit significant $CaCO_3$ contents and a predominantly loamy texture along the entire profile.

This is consistent with the fine grain size (< 50 µm) typically observed in Thalassossols, and in the ploughed soils of the Wateringues marine plain (Sterckeman et al., 2004). In addition, $CaCO_3$ and CaO concentrations are highly correlated (R= 0.97), suggesting a dominance of calcium as carbonates in these soils. This hypothesis is further supported by both the pH values, which reflect neutral to slightly basic conditions (Luo et al., 2015), and the global mineralogical composition of the studied soils.

3.1.3 Principal Component Analysis: pattern analysis of soil cores

The physicochemical parameters of soil samples revealed significant differences between the soil cores and depths. A Principal Component Analysis (PCA) was performed on the physicochemical data set (Fig. 4). PCA showed that the two first principal components contributed to 78.4 % of the total variance. The first principal component (PC1, 56.2 %) is mainly formed by SiO_2, Al_2O_3, CaO and Fe_2O_3 contents and distinguishes soil cores based on their global mineralogical composition, as previously described: sandy loam texture with a dominance of SiO_2 and quartz, in cores 1 and 2; Silty loam texture with higher Al_2O_3, Fe_2O_3, CaO concentrations and clayey fractions, in cores 3 and 4. Illite is dominant in cores 1 and 2, whereas smectite is the main clay mineral detected in cores 3 and 4. The second principal component (PC2, 22.2 %), composed of TOC, water content and CEC, mostly separates subsurface samples from deep samples on cores 2, 3 and 4.

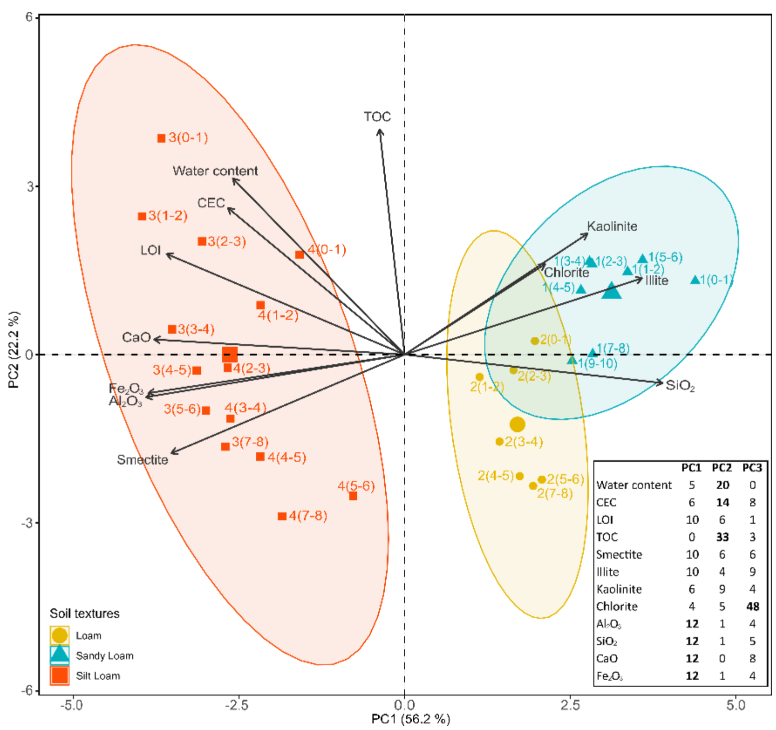

Figure 4: Principal component analysis (PCA) illustrating the variations of the pedological variables (arrows) for all the soil cores from Gravelines city and textures (colored symbols). Three domains (ellipses) correspond to the different textures of soils and

highlight distinct cores, depths and behaviors. Larger symbols indicate the centroid of values for each soil texture. The percentage of contribution of the different pedological variables in the building of the PCA axis is inset (bottom right). The most important contributors are denoted in bold.

3.2 Vertical PTE concentrations in soil cores

3.2.1 Total PTE concentrations

PTE concentrations, measured along the four soil cores, are presented in Table 3. Results indicate variations in PTE concentrations between the studied cores, and higher concentrations in some PTE compared to the ploughed soils of the so-called Wateringues marine plain (Sterckeman et al., 2004). Core 1 presents the lowest average concentrations for all the analyzed PTE, except Mo (0.4 $mg.kg^{-1}$). A significant vertical evolution is only observed for this element, increasing from 0.3 $mg.kg^{-1}$ in the deepest layer to 0.5 $mg.kg^{-1}$ in the subsurface. For the other cores, all the PTE concentrations are higher in the subsurface. Core 2 exhibits intermediate average values of 34, 257 and 10 $mg.kg^{-1}$ for Cr, Mn and Ni, respectively. This core is also characterized by the highest average Cu concentrations (10 $mg.kg^{-1}$) and the lowest average Mo concentrations (0.3 $mg.kg^{-1}$). Core 3 is characterized by the highest average concentrations in Cr, Mn, Ni, Mo and Zn (with 57, 326, 17, 0.8 and 60 $mg.kg^{-1}$, respectively) and the lowest average concentrations in Cu (7 $mg.kg^{-1}$). Cr, Ni, Mo and Zn values are more than twice higher than the Wateringues marine plain background (Sterckeman et al., 2004) in the subsurface of this core. Finally, core 4 presents the same pattern as core 3 in average, but with slightly lower values. Values more than twice higher than the Wateringues marine plain background were observed only for Mo and Zn with concentrations higher than 0.3 and 71 $mg.kg^{-1}$, respectively.

Table 3: Evolution of PTE contents with depths of the four soil cores collected in Gravelines ($mg.kg^{-1}$). Values more than twice higher than the Wateringues marine plain background (median values) are denoted in bold. SD: Standard Deviation. N.d.: not determined; "-" means no data. (a) Sterckeman et al., 2004.

Core	Depth (cm)	Cr	Mn	Ni	Cu	Zn	Mo	Cd
1	0-1	22	102	8	7	39	**0.5**	0.16
	1-2	22	103	8	8	41	**0.5**	0.16
	2-3	24	109	8	8	45	**0.5**	0.17
	3-4	22	107	8	8	**72**	**0.4**	0.19
	4-5	22	103	8	8	44	**0.4**	0.17
	5-6	21	105	8	8	41	**0.4**	0.18
	7-8	21	105	8	8	41	0.3	0.20
	9-10	-	-	-	-	-	-	-
	10-11	24	106	8	8	40	0.3	0.18
	Average	22	105	8	8	45	0.4	0.18
	SD	1	2	0.2	0.3	10	0.1	0.01
2	0-1	37	278	11	11	67	**0.6**	0.39
	1-2	36	265	11	10	63	**0.5**	0.34
	2-3	30	276	10	11	63	0.2	0.33
	3-4	33	250	10	12	64	0.2	0.33
	4-5	34	254	10	11	56	0.2	0.31

Core	Depth (cm)	Cr	Mn	Ni	Cu	Zn	Mo	Cd
	5-6	35	255	10	9	54	0.3	0.34
	7-8	33	240	10	9	55	0.2	0.32
	9-10	-	-	-	-	-	-	-
	10-11	33	240	9	9	47	0.2	0.33
	Average	34	257	10	10	59	0.3	0.34
	SD	2	14	0.5	1	6	0.1	0.02
3	0-1	**67**	381	**22**	9	**90**	**1.4**	0.42
	1-2	**63**	335	**19**	8	**73**	**0.9**	0.42
	2-3	**60**	333	**18**	8	68	**0.9**	0.40
	3-4	**57**	322	17	8	58	**0.7**	0.39
	4-5	**57**	321	16	7	53	**0.7**	0.38
	5-6	55	308	16	7	50	**0.6**	0.33
	7-8	52	299	15	7	47	**0.6**	0.34
	9-10	-	-	-	-	-	-	-
	10-11	49	308	14	6	45	**0.4**	0.30
	Average	57	326	17	7	60	0.8	0.37
	SD	5	24	2	1	14	0.3	0.04
4	0-1	42	300	13	9	56	**0.6**	0.24
	1-2	41	281	13	9	**77**	**0.6**	0.23
	2-3	41	282	12	9	47	**0.5**	0.24
	3-4	41	292	12	9	45	**0.4**	0.23
	4-5	45	292	12	9	43	**0.4**	0.23
	5-6	40	290	12	9	43	0.3	0.21
	7-8	38	279	11	8	40	0.3	0.21
	9-10	-	-	-	-	-	-	-
	10-11	38	274	12	8	40	0.2	0.20
	Average	41	286	12	9	49	0.4	0.22
	SD	2	8	0.5	0.5	11	0.1	0.01
Total average		39	244	12	9	53	0.5	0.28
SD		13	86	4	1	13	0.3	0.09
Wateringues marine plain background (a)		28	207	9	7	36	0.2	0.24

3.2.2 PTE ratios of HCl leached fractions

Table 4 displays the leached fraction results for PTE along depth for the four soil cores (concentrations and leached ratios (leached/total in %)). The studied PTE present different average of leached ratios, increasing as follows: Cr (7 %), Mo (11 %), Ni (25 %), Zn (43 %), Cu (47 %), Mn (62 %) and Cd (68 %). For all the studied PTE, the lowest leached ratios are calculated for core 3. An opposite trend is observed for core 2. Globally, the leached ratios of PTE present no specific variation on the vertical profiles.

Table 4: Leached concentrations (mg.kg^{-1}) and leached ratios (leached concentration/total concentration in %) of the studied PTE in the 4 soil cores, after HCl 1M extraction. SD: Standard Deviation. N.d.: not determined. "-" means no data.

		Leached concentrations (mg.kg^{-1})							Leached ratios (%)						
Core	Depth (cm)	Cr	Mn	Ni	Cu	Zn	Mo	Cd	Cr	Mn	Ni	Cu	Zn	Mo	Cd
1	0-1	2	60	2	4	21	0.05	0.12	8	59	28	51	54	11	75

		Leached concentrations (mg.kg^{-1})							Leached ratios (%)						
Core	Depth (cm)	Cr	Mn	Ni	Cu	Zn	Mo	Cd	Cr	Mn	Ni	Cu	Zn	Mo	Cd
	1-2	2	67	2	4	23	0.04	0.12	8	64	28	53	56	9	75
	2-3	2	68	2	4	23	0.04	0.13	7	62	27	52	52	8	76
	3-4	2	68	2	4	25	0.04	0.14	7	63	28	52	-	9	74
	4-5	2	64	2	4	23	0.03	0.14	7	62	28	51	52	7	82
	5-6	2	64	2	4	22	0.03	0.13	7	61	27	53	54	8	72
	7-8	2	65	2	4	22	0.03	0.13	8	61	28	53	53	10	65
	9-10	-	-	-	-	-	-	-	-	-	-	-	-	-	-
	10-11	2	60	2	4	20	0.02	0.13	6	56	25	52	49	6	72
	Average	2	64	2	4	22	0.04	0.13	7	61	27	52	53	8	74
	SD	0	3	0	0	1	0.01	0.01	1	2	1	1	2	1	5
2	0-1	3	166	3	6	35	0.07	0.26	8	60	25	53	52	13	67
	1-2	3	163	3	6	34	0.07	0.24	9	62	26	54	54	15	71
	2-3	3	167	3	6	33	0.06	0.24	11	60	26	54	51	29	73
	3-4	4	163	3	6	34	0.04	0.22	11	65	28	53	53	17	67
	4-5	3	160	3	6	27	0.04	0.21	10	63	26	54	49	24	68
	5-6	3	151	3	5	25	0.03	0.21	9	59	26	52	46	12	62
	7-8	3	161	3	5	27	0.03	0.22	10	67	27	55	50	14	69
	9-10	-	-	-	-	-	-	-	-	-	-	-	-	-	-
	10-11	3	154	3	5	23	0.03	0.21	10	64	27	56	49	14	64
	Average	3	161	3	6	30	0.05	0.23	10	63	26	54	50	17	67
	SD	0	5	0	0	4	0.02	0.02	1	3	1	1	2	6	3
3	0-1	4	222	5	4	43	0.14	0.26	6	58	21	41	48	10	62
	1-2	4	208	4	4	35	0.09	0.26	6	62	23	43	48	10	62
	2-3	3	192	3	3	27	0.09	0.24	5	58	19	38	40	11	60
	3-4	3	196	3	3	22	0.08	0.23	5	61	19	40	39	11	59
	4-5	3	195	3	3	20	0.08	0.22	6	61	21	40	38	12	58
	5-6	3	186	3	3	17	0.06	0.20	5	60	19	39	34	10	61
	7-8	3	178	3	3	15	0.06	0.20	6	60	19	38	32	10	59
	9-10	-	-	-	-	-	-	-	-	-	-	-	-	-	-
	10-11	3	177	3	2	14	0.06	0.18	6	58	20	35	31	14	60
	Average	3	194	3	3	24	0.08	0.22	6	60	20	39	39	11	60
	SD	0	14	1	0	10	0.02	0.03	0	2	1	2	6	1	1
4	0-1	3	191	4	4	22	0.05	0.17	7	64	30	43	39	8	71
	1-2	3	178	4	4	20	0.05	0.17	7	63	28	42	26	8	74
	2-3	3	178	3	4	17	0.04	0.17	7	63	27	41	37	8	71
	3-4	3	179	3	4	16	0.03	0.16	7	61	27	43	36	7	70
	4-5	3	186	3	4	14	0.03	0.15	6	64	27	42	33	8	65
	5-6	3	177	3	4	13	0.03	0.15	7	61	25	40	31	10	71
	7-8	3	175	3	3	13	0.02	0.14	7	63	26	41	32	7	67
	9-10	-	-	-	-	-	-	-	-	-	-	-	-	-	-
	10-11	3	178	3	3	13	0.01	0.15	8	65	26	38	33	4	75
	Average	3	180	3	4	16	0.03	0.16	7	63	27	41	35	8	70
	SD	0	5	0	0	3	0.01	0.01	0	1	2	1	3	2	3
Total average		3	150	3	4	23	0.05	0.18	7	62	25	47	44	11	68
SD		1	52	1	1	8	0.03	0.05	2	2	3	7	9	5	6

4 Discussion

4.1 Qualitative reactivity of soil cores toward PTE

4.1.1 Reactivity of organic matter in the studied soils

The results of the Van Krevelen diagram (Fig. 2) suggest that the organic carbon detected in the studied soils is predominantly in the form of fulvic acids. This point may be explained by the presence of calcium carbonate in the studied soils, which is considered to stabilize lowly polymerized humic substances such as fulvic acids (Duchaufour, 1970; Duchaufour et al., 2020). This kind of humic substance is particularly soluble and has an adsorption capacity for metals that is 2-20 times higher than humic acids, due to their greater amount of reactive functional groups (carboxyl, phenolic, carbonyl…) (Donisa et al., 2003; Borůvka and Drábek, 2004; dos Santos et al., 2020). Futhermore, previous studies showed that pH values ranging from 6 to 8 tend to stabilize metal ions in soils by forming water-insoluble acid fulvic complexes (Schnitzer and Kerndorff, 1981; Boguta and Sokołowska, 2020). These results suggest a potential stabilization of PTE inputs by the organic matter of the studied soils, especially under the current acido-basic conditions (average pH value : 7.8). Thus, a significant change in the pH values could favor the mobilization of PTE. While the organic carbon in the studied soils predominantly occurs as fulvic acids (without significant variations between cores and with depth), the pedological properties of the cores (Table 2) reveal notable differences that could influence their reactivity and the behavior of their absorbent complex.

4.1.2 Discrimination of cores by the reactivity of their absorbent complex

The results of the PCA (Fig. 4) reveal that the soil cores and depths can be distinguished by their mineralogical composition (PC1) and physicochemical properties (PC2), which may influence their capacity to retain metallic contaminants and thus their fate in the environment (Fijałkowski et al., 2012; Campillo-Cora et al., 2020; Yu et al., 2023). Focusing on the first principal component, previous studies highlighted the importance of smectite in soil absorption capacities (Varadachari et al., 1994; Hanna et al., 2009; Orucoglu et al., 2022) due to their specific surface area and their influence on CEC values (Otunola and Ololade, 2020). This observation is consistent with the higher proportion of smectite detected in cores 3 and 4, presenting a higher sorption capacity than cores 1 and 2. The second principal component describes the sorption efficiency of the clay-humus soil complex through organic compounds and the presence of fine-grained materials (Warwick et al., 1998; Bronick and Lal, 2005; Hernandez-Soriano and Jimenez-Lopez, 2012). This component mostly discriminates subsurface samples from deep samples on cores 2, 3 and 4, reflecting the enhanced retention capacity of contaminants near the soil surfaces (Fiedler et al., 2007; Chitolina et al., 2020). By combining the two principal components, the PCA differentiates the soil cores and depths based on the potential retention capacity of their absorbent complex (Impellitteri et al., 2002; Bradl, 2004; Lasota et al., 2020). The subsurface samples of cores 3 and 4 (nearest to the industrial emitters) present the highest sorption capacities compared to the deeper ones. Core 2 (intermediate location between industries and city center) presents the same pattern but with a globally lower sorption capacity than cores 3 and 4. Core 1 (in the city center) exhibits the lowest sorption capacities with a notable homogeneity with depth.

4.2 Soil contaminations by industrial or urban PTE inputs

4.2.1 Highlighting atmospheric PTE inputs in the soils of Gravelines

Enrichment factors (EF) were calculated for Cr, Mn, Ni, Cu, Zn, Mo and Cd by comparing the soils of Gravelines to those of the surrounding Wateringues marine plain and normalizing to Al contents (Fig. 5). Core 1 was not considered because of its Al concentrations below the detection limit. According to Chen et al. (2007) the cores 2, 3 and 4 can be globally described by minor PTE enrichments (1 < EF < 3, Fig. 5) except for Mo (punctual moderately severe enrichments, with 5 < EF < 10). As suggested in a previous study (Casetta et al., 2024), the present PTE values and EF support the hypothesis of a diffuse contamination of the soils of Gravelines. Furthermore, vertical profiles of enrichment factors show that the slight PTE accumulations in cores 2 (Cr, Mn, Ni, Cu, Zn, Mo, Cd), 3 (Cr, Ni, Zn, Mo) and 4 (Zn, Mo) mostly occur within the two first cm. As reported in numerous studies (Williams et al., 1987; Li and Shuman, 1996; Sterckeman et al., 2000), these patterns of superficial accumulation suggest atmospheric and anthropogenic PTE inputs, particularly in cores 2 and 3.

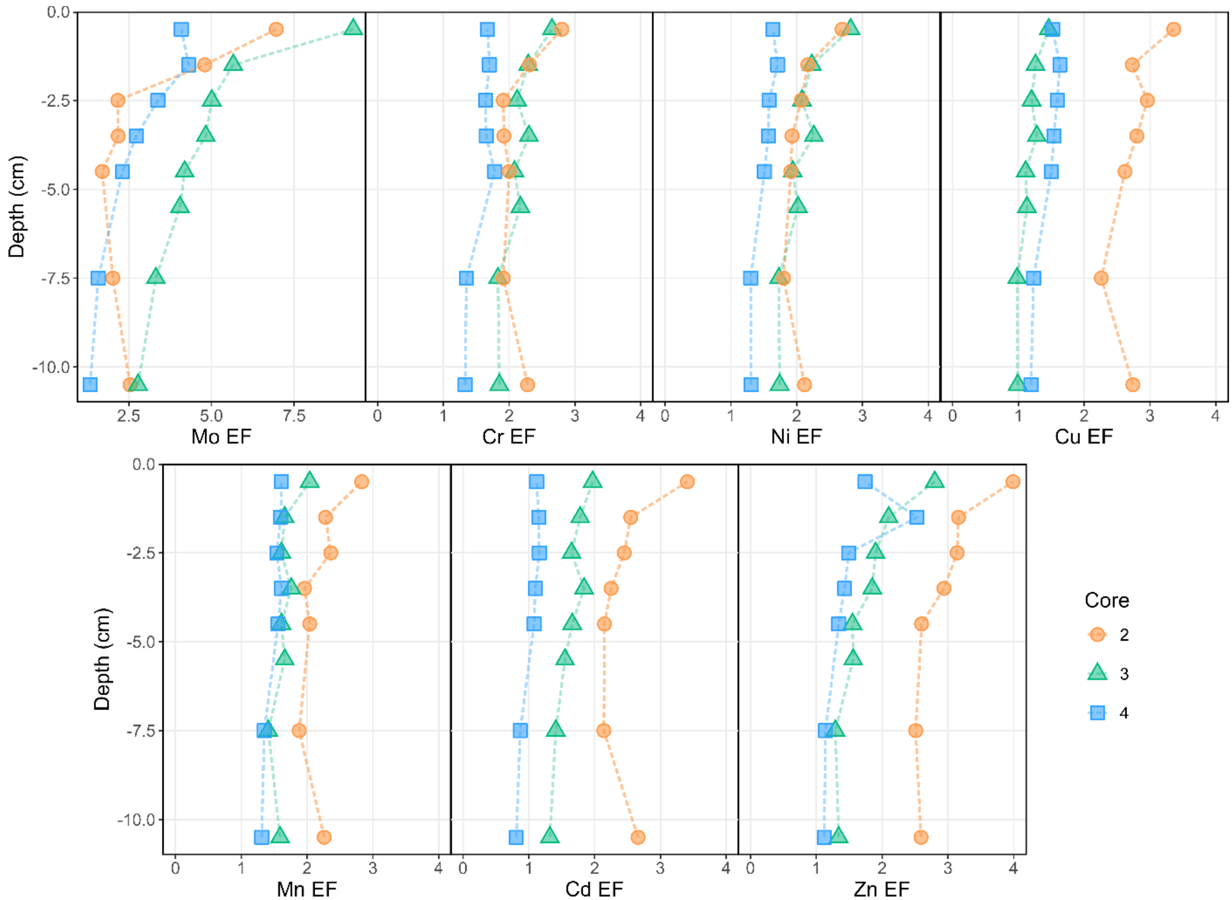

Figure 5: Vertical profiles of Cr, Mn, Ni, Cu, Zn, Mo and Cd enrichment factors (against Al) in cores 2, 3 and 4. Reference materials corresponds to the median values obtained on the Wateringues marine plain soils (Sterckeman et al., 2004)

4.2.2 Are the PTE inputs in stations 2 and 3 related to industrial dust?

The previous characterization of dust fallout collected in Gravelines revealed high enrichment in some PTE, compared to the upper continental crust and using Sc as immobile element (Taylor and McLennan, 1995): EF(Cr) = 108, EF(Mn) = 36, EF(Ni) = 78, EF(Zn) = 60, EF(Mo) = 169, EF(Cd) = 235 (Casetta et al., 2024). As Cu (with EF < 20) may originate from multiple sources in such an urban environment (roof, garden and lawn treatment, car brakes; Panagos et al., 2018), it will not be used to trace industrial inputs. Considering these results and other studies carried out on the atmospheric particles emitted in the Dunkerque agglomeration (Alleman et al., 2010; Hleis et al., 2013; Kfoury et al., 2016), a metallurgical dust influence could explain the chemical signatures of the soil cores 2 and 3 from two points of view: (1) the slight but notable accumulation of Mo, Cr and Ni in the subsurface of soil cores 2 and 3; and (2) the same pattern of accumulation of Mn, Zn and Cd, three other PTE associated with industrial activities. For the core 3, this hypothesis is also supported by the strong correlations calculated between its Mo, Cr and Ni enrichment factors (R > 0.93) and its Mn, Cd and Zn enrichment factors (R > 0.81). In contrast, these correlations are significantly lower for the core 2. This trend of high correlations between the studied PTE (e.g. R > 0.97 for Cr and Ni EF) is globally observed for the all data set (Table 5). Based on this interpretation and on the calculated EF (Fig. 5), both cores seem to be influenced by Cr, Ni and Mo inputs but core 2 appears more impacted by Mn, Zn and Cd inputs than core 3. Considering Cr as the less mobile PTE in the studied soils (Table 4), the use of some PTE against Cr ratios (Zn/Cr vs 100Cd/Cr and Cr/Mo vs Ni/Mo, Fig. 6) allowed us to visualize and highlight these two different anthropogenic signatures in the considered soil cores, according to depth. Thus, core 3 samples present a chemical signature close to the studied dust data (Fig. 6a). The signature is different for core 2 samples, with the highest considered PTE ratios. Cr/Mo and Ni/Mo ratios (Fig. 6b) underline that the core 2 subsurface samples are marked by the chemical signature highlighted in core 3. Knowing the diversity of atmospheric emissions from metallurgical activities in the studied area (Alleman et al., 2010; Hleis et al., 2013; Registre des émissions polluantes, 2023; Pollution des sols, SIS et anciens sites industriels, 2023), the presence of different industrial chemical signatures in soils is not surprising.

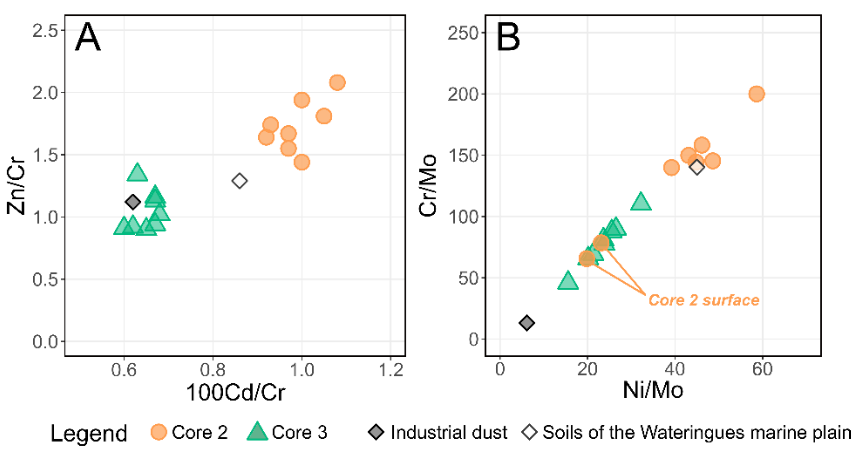

Figure 6: Elemental ratio diagrams for cores 2 and 3, industrial bulk dust and median Wateringues maritime plain soils. (A) Zn/Cr vs 100Cd/Cr and (B) Cr/Mo vs Ni/Mo.

No statistically-significant correlation was observed between the calculated EF and the distance from the emission sources, as previously observed with more topsoil samples in Gravelines (Casetta et al., 2024). According to this latter study and regarding the spatial location of the current soil cores, the highest EF measured on core 2 seem to be mostly related to the soil exposure, i.e. the absence of vegetal or urban protecting barriers. Concerning Mn, Cu, Zn and Cd concentrations, urban influences in soils cannot be excluded, considering the potential emission of Mn, Cu and Zn by non-exhaust road traffic (Smolders and Degryse, 2002; Lee et al., 2006; Guo et al., 2012) as well as the correlation between their enrichment factors in soils (R=0.81, Table 5). Likewise, the use of Cu and Cd as pesticide or Mn and Cd occurrence in fertilizers and compost (Baize, 1997; Campos, 2003; He et al., 2005) remains possible.

Table 5: Spearman's correlation matrix (R values) of pedological parameters, PTE-EF and HCl leached ratios in the studied soil cores (bold values represent significant correlations with R > 0.80 and p < 0.05). CEC: Cationic Exchange Capacity; TOC: Total Organic Carbon. EF: Enrichment factor.

	Water content	CEC	TOC	Al_2O_3	SiO_2	CaO	Fe_2O_3	EF.Cr	EF.Mn	EF.Ni	EF.Cu	EF.Zn	EF.Mo	EF.Cd	% leached Cr	% leached Mn	% leached Ni	% leached Cu	% leached Zn	% leached Mo	% leached Cd
Water content	**1.00**																				
CEC	**0.83**	**1.00**																			
TOC	**0.81**	0.66	**1.00**																		
Al_2O_3	0.07	0.23	-0.30	**1.00**																	
SiO_2	-0.39	-0.40	0.03	**-0.86**	**1.00**																
CaO	0.17	0.25	-0.24	**0.92**	**-0.90**	**1.00**															
Fe_2O_3	0.07	0.23	-0.35	**0.94**	**-0.82**	**0.94**	**1.00**														
EF.Cr	0.08	-0.10	0.20	-0.47	0.09	-0.14	-0.41	**1.00**													
EF.Mn	-0.19	-0.36	-0.01	**-0.84**	0.51	-0.61	-0.78	0.80	**1.00**												
EF.Ni	0.13	-0.03	0.31	-0.47	0.05	-0.14	-0.43	**0.97**	**0.81**	**1.00**											
EF.Cu	-0.33	-0.43	-0.12	**-0.93**	**0.81**	**-0.89**	**-0.84**	0.32	0.75	0.34	**1.00**										
EF.Zn	-0.07	-0.27	0.19	**-0.82**	0.50	-0.64	-0.80	0.70	**0.90**	0.73	**0.81**	**1.00**									
EF.Mo	0.77	0.59	0.79	0.03	-0.51	0.28	0.03	0.58	0.20	0.60	-0.13	0.29	**1.00**								
EF.Cd	-0.25	-0.49	-0.02	-0.72	0.45	-0.44	-0.61	0.80	**0.87**	0.79	0.63	**0.87**	0.24	**1.00**							
% leached Cr	-0.67	-0.67	-0.39	-0.45	0.61	-0.54	-0.40	-0.07	0.44	-0.07	0.79	0.47	-0.60	0.40	**1.00**						
% leached Mn	-0.16	-0.05	-0.05	-0.02	0.19	-0.17	-0.00	-0.46	-0.19	-0.49	0.28	-0.08	-0.52	-0.20	0.47	**1.00**					
% leached Ni	-0.08	-0.09	0.23	-0.53	0.61	-0.65	-0.52	-0.44	-0.01	-0.43	0.55	0.15	-0.43	-0.11	0.55	0.66	**1.00**				
%leached Cu	-0.37	-0.50	-0.04	-0.72	0.69	-0.67	-0.64	0.28	0.66	0.26	**0.86**	0.74	-0.15	0.63	0.76	0.31	0.49	**1.00**			
% leached Zn	-0.12	-0.31	0.28	-0.77	0.70	-0.73	-0.76	0.53	0.71	0.52	0.65	0.78	0.12	**0.81**	0.49	0.05	0.41	0.76	**1.00**		
% leached Mo	-0.31	-0.54	-0.38	-0.01	-0.09	0.08	-0.05	0.53	0.69	0.51	0.49	0.68	-0.06	**0.83**	0.33	-0.14	-0.22	0.34	0.21	**1.00**	
% leached Cd	-0.08	-0.02	0.32	-0.57	0.62	-0.75	-0.64	-0.41	0.05	-0.34	0.49	0.15	-0.38	-0.22	0.38	0.37	0.69	0.36	0.36	-0.44	**1.00**

4.3 Mobility of PTE in the soils of Gravelines

Assessing the impact of industrial dust on the environment partly stands on the mobility of their dust-borne metals in soils. Thus, the general mobility of PTE in contaminated soils (particularly cores 2 and 3) was estimated using 1M HCl single extraction. Easy to manage, this kind of extraction is often performed on different types of sediment (Hamdoun et al., 2015; Yu et al., 2021) in order to assess the bio-accessible fraction of a specific metal content (Snape et al., 2004; Philippe et al., 2008; Roosa et al., 2016). HCl is prone to extract the labile fraction (exchangeable, bound to calcium carbonate, part of oxides and to acid volatile sulfides) (Billon, 2001; Townsend et al., 2007; Waterlot et al., 2017; Pelfrêne et al., 2020). Considering the studied soils, particularly rich in calcium carbonates (12 to 30 %), the use of 1M HCl with a prolonged reaction time was required to avoid underestimating the buffering effect of carbonates, as described in the methodology. Based on these considerations, this HCl extraction highlights the mobility of specific PTE under local pH changes. Literature data summarized in the Table 1 show that a high mobility for Cu, Mn, Mo, Ni, Zn and in a lesser extent Cd, and a low mobility for Cr can be expected after HCl 1M leaching of the studied soils

4.3.1 Comparison of the different stations

As observed for PTE concentrations, no significant evolution of PTE leached ratios (leached/total content) was observed in the vertical profiles of the four soil cores (according to their SD values) (Table 4). Moreover, PTE leached ratios remain stable even at the subsurface despite the occurrence of organic matter. These results are consistent with the observed lack of correlation between the PTE leached fractions and TOC contents (Table 5). The soil core collected in station 1 (city center) is characterized by the less efficient absorbent complex (Fig. 4) and the lowest total PTE concentrations (Table 3). However, Cu, Zn and Cd (known as more mobile when coming from mixed anthropogenic sources (Baize, 1997)) were the most extracted PTE in this station (Table 4). Thus, these results reveal a classical urban PTE contamination in the city center (station 1). The soil core collected in station 4 presents higher absorbent capacities (Fig. 4) and higher PTE total concentrations in Cr, Mn, Ni and Mo compared to the soil cores 1 and 2 (Table 3). The correlation between total PTE concentrations may reflect an industrial signature (Cr, Mn, Ni, Mo) on these soils despite the relatively low PTE EF (Fig. 5). Compared to the other cores, the leached ratios are average for Cr-Mn-Ni and slightly lower for Cu-Zn-Mo (Table 4). This could be related to (1) the soil properties (rich in clay fraction), (2) the relatively lower solubility of PTE from industrial dust or (3) both. The important Cd leached fraction (70 %) is however noticeable (Table 4). This result is of concern regarding the presence of allotment gardens close to station 4. The highest PTE EF, in particular at surface, are measured in the soil cores 2 and 3 (Fig. 5). The superficial PTE accumulations on these stations (located close to the industrial emitters) were previously related to industrial and atmospheric inputs (see section 4.2.2). As the present study aims to discuss the ecotoxicological impact of industrial dust deposition on urban soils, the following parts focus on the PTE leached ratios in these cores 2 and 3.

4.3.2 Mobility of all the studied PTE in cores 2 and 3

In the soil cores 2 and 3, Mn, Cu, Zn and Cd appear rather mobile compared to Cr, Ni and Mo (Table 4). The mobility of the first group of elements (average leached values both > 39 %) in presence of HCl 1M is not surprising considering their natural mobility in oxidant and/or acidic conditions (Table 1).The high mobility of Mn and Cd (average leached values > 60 %) can be additionally explained by (1) their natural association to the exchangeable and calcium carbonates fractions in soils (Table 1, Ren et al., 2015; Kubier et al., 2019), and (2) the concentration of carbonate calcium (easily dissolved by HCl 1M) in these soils (ranging 12 to 28 %). Concerning now the second group of elements, low Cr leached ratios are consistent with the natural behavior of this PTE in soils (Table 1) and may indicate the association of this element with anthropogenic or natural refractory phases (Fendorf, 1995). Ni and Mo naturally present strong affinities with calcium carbonates, organic matter and Fe/Mn oxides (Shi et al., 2012; Bielefeldt and Vos, 2014; King et al., 2018). They are expected to be particularly mobile under oxidant and acidic conditions (Table 1). Despite the use of HCl 1M treatment, the moderately low Ni and Mo leached ratios (< 27 % for Ni and < 17 % for Mo) suggest their association with anthropogenic or natural (iron oxides, silicates) refractory phases (specific adsorption on organic matter or inclusion in mineralogical phases) (Bibak et al., 1994; Goldberg et al., 1996; Gardner et al., 2012; Barman et al., 2015).

4.3.3 Specific mobility of industrial dust-borne PTE in cores 2 and 3

The four dominant types of industrial dust fallout identified in the city of Gravelines (coal particles, slags, iron ores and aluminum oxides) are the main bearing phases of several PTE, including Cr, Ni, Mo, Zn, Cd and Mn (Casetta et al., 2024). In light of current knowledge, it is not possible to relate a PTE to a specific bearing phase. As Cr, Ni and Mo are supposed to be present in soils within refractory phases, the hypothesis of an industrial nature of these latter in cores 2 and 3 is supported by (1) the previously described Cr, Ni and Mo enrichment factors and (2) the known low mobility of Cr and Ni found in industrial coals and slags (Cabrera-Real et al., 2012; Albertsson et al., 2014; Mombelli et al., 2016; Zhao et al., 2018; Feng et al., 2000). The high mobility of Mn, Zn and Cd in cores 2 and 3 is consistent with previous studies focused on their mobility in industrial coals and slags (Fernández-Turiel et al., 1994; Querol et al., 1995; Han et al., 2019; Li et al., 2020; Kicińska, 2021). Regarding the absence of significant correlations between the Mn and Cd EF and their leached ratios, it is however complicated to draw conclusion about their origin, chemical form and subsequent behavior in the soil cores. Only Zn presents a positive correlation between total content and leached ratios (R = 0.78), suggesting the higher mobility of this element from anthropogenic inputs.

Thus, the study tends to reveal the stability of industrial dust bearing Cr, Ni and Mo in soils, as these PTE were lowly leached despite the use of a powerful extraction reagent (HCl 1M). These results highlight a relative immobility of these harmful elements in the environment (Smedley and Kinniburgh, 2017; DesMarais and Costa, 2019) and then their low bioavailability. Nevertheless, this stability does not eliminate the potential environmental and sanitary risks. The accumulation of these PTE in the soil subsurface layer, combined with changes in environmental conditions such as pH or redox potential, could increase their mobility. As the studied soils latter are developed at low altitude (0-25 m), their vulnerability in the context of ongoing sea level rise is particularly significant. Flooding events, which could become more frequent due to rising sea levels, could affect soil salinity and redox conditions, potentially releasing these stable contaminants into the environment (Hailegnaw et al., 2024; Pellegrini et al., 2024). Additionally, the use of these soils for allotment gardens near industrial emitters poses a risk of human exposure to contaminants through the cultivation of vegetables or soil contact, especially for children (Calabrese et al., 1997; Crispo et al., 2021).Thus, while our results suggest limited immediate mobility of Cr, Ni, and Mo, a monitoring of environmental changes and their effects on these PTE is recommended for assessing long-term environmental and sanitary risks.

5 Conclusion

The main challenge of this study was to evaluate the vertical distribution and mobility of PTE in the soils of Gravelines, mainly derived from the deposition of industrial dusts. Although the studied soils globally present minor PTE enrichments, specific levels of contamination were identified in the soil cores. These were related to industrial dust deposition through (1) the higher PTE concentrations and EF in the core subsurface (0-3 cm), suggesting anthropogenic and atmospheric inputs of the contaminants, and (2) the significant associations of metallurgical tracer elements, as Cr-Ni-Mo or Mn-Zn-Cd. The assessment of the general mobility of industrial PTE in soils reveals the stability of Cr, Ni and Mo, despite the use of a relatively strong extractant (HCl 1M) and suggests their association to industrial refractory phases such as coals and slags. Conversely, Mn, Zn and Cd have a higher mobility. Knowing that HCl 1M extraction destabilizes the exchangeable, carbonated, organic and oxide soil fractions, these PTE could not be only related to metallurgical particles.

The calcareous soils of Gravelines globally present low absorbent capacities, partially counterbalanced by their buffering capacities. In case of destabilization of industrial dust in soils, these results highlight that the released ions (especially Cr, Ni and Mo) would be more retained in soils with more efficient absorbent complex and significant carbonate contents (e.g. core 3 vs core 2). Then, the present study shows the importance of studying pedological parameters (texture, mineralogy, TOC, water content, CEC) to understand their influence on the PTE concentrations and to evaluate their mobility. In the future, however, interactions between soil and other environmental compartments are likely to be disrupted by climate change. This could increase particle weathering (e.g. carbonate, oxides) and consequently induce higher mobility of some PTE (Hailegnaw et al., 2024; Pellegrini et al., 2024). This hypothesis must be particularly considered, regarding (1) the potential toxicity of these elements in their mobile form, (2) their accumulation in the soil subsurface, which interacts with all the environmental compartments and (3) the possible PTE contamination of food produced in the urban allotment gardens (near the industrial emitters) and consumed by local inhabitants.

Code/Data availability

All the data used in this study are presented in the tables and supplementary materials.

Author contribution

Marine Casetta: Conceptualization, Data curation, Formal analysis, Investigation, Methodology, Validation, Visualization Writing—Original Draft preparation, Writing—Review & Editing; Sylvie Philippe: Conceptualization, Funding acquisition, Investigation, Methodology, Project administration, Resources, Supervision, Validation, Writing—Review & Editing; Lucie Courcot: Conceptualization, Investigation, Methodology, Supervision, Validation, Writing—Review & Editing; David Dumoulin: Investigation, Validation, Writing—Review & Editing; Gabriel Billon: Validation, Writing—Review & Editing;

François Baudin: Investigation, Validation, Writing—Review & Editing; Françoise Henry: Investigation, Resources, Validation, Writing—Review & Editing; Michaël Hermoso: Resources, Supervision, Writing—Review & Editing; Jacinthe Caillaud: Conceptualization, Funding acquisition, Investigation, Methodology, Project administration, Resources, Supervision, Validation, Writing—Review & Editing;

Competing interests

The authors declare that they have no conflict of interest.

Acknowledgements

The leading author thank the Pôle Métropolitain Côte d'Opale (PMCO) and the Region Hauts-de-France for providing a PhD scholarship. The French government and the Region Hauts-de-France are warmly acknowledged for the co-funding of the project (CPER Climibio and CPER MARCO). This study was also supported by the EC2CO project (INSU CNRS) and the SFR Campus de la mer. ICP-AES/MS and XRD analyses were performed on the Chevreul Institute Platform (U-Lille/CNRS) and the Platform CARMIN – Ulille infrastructure, respectively. The authors would like to thank Véronique Alaimo and Marion Delattre for their technical support and assistance in these analyses. Thanks to Laurine Hopf and Louise Legrand who provided helpful technical assistance in the laboratory during their trainees. Authors also thank the agglomeration of Dunkerque, the city of Gravelines, the DREAL, SPPPI and ALOATEC structures. We finally wanted to thank the two anonymous reviewers for their constructive comments that helped to improve the paper.

References

Albertsson, G. J., Engström, F., and Teng, L.: Effect of the Heat Treatment on the Chromium Partition in Cr-Containing Industrial and Synthetic Slags, steel research international, 85, 1418–1431, https://doi.org/10.1002/srin.201300231, 2014.

Alleman, L. Y., Lamaison, L., Perdrix, E., Robache, A., and Galloo, J.-C.: PM10 metal concentrations and source identification using positive matrix factorization and wind sectoring in a French industrial zone, Atmospheric Research, 96, 612–625, https://doi.org/10.1016/j.atmosres.2010.02.008, 2010.

Amar, M., Benzerzour, M., Kleib, J., and Abriak, N.-E.: From dredged sediment to supplementary cementitious material: characterization, treatment, and reuse, International Journal of Sediment Research, 36, 92–109, https://doi.org/10.1016/j.ijsrc.2020.06.002, 2021.

Aran, D., Maul, A., and Masfaraud, J.-F.: A spectrophotometric measurement of soil cation exchange capacity based on cobaltihexamine chloride absorbance, Comptes Rendus Geoscience, 340, 865–871, https://doi.org/10.1016/j.crte.2008.07.015, 2008.

Baize, D.: Teneurs totales en éléments traces métalliques dans les sols (France), INRA Editions, Paris, 408 pp., 1997.

Baize, D. and Girard, M.-C.: Référentiel pédologique, [Éd.] 2008., Éd. Quae, Versailles, 2009.

Balaria, A., Johnson, C. E., and Xu, Z.: Molecular-Scale Characterization of Hot-Water-Extractable Organic Matter in Organic Horizons of a Forest Soil, Soil Science Society of America Journal, 73, 812–821, https://doi.org/10.2136/sssaj2008.0075, 2009.

Barman, M., Datta, S. P., Rattan, R. K., and Meena, M. C.: Chemical fractions and bioavailability of nickel in alluvial soils, Plant, Soil and Environment, 61, 17–22, https://doi.org/10.17221/613/2014-PSE, 2015.

Bibak, A., M∅berg, J. P., and Borggaard, O. K.: Content and Distribution of Cobalt, Copper, Manganese and Molybdenum in Danish Spodosols and Ultisols, Acta Agriculturae Scandinavica, Section B — Soil & Plant Science, 44, 208–213, https://doi.org/10.1080/09064719409410247, 1994.

Billon, G.: Géochimie des métaux et du soufre dans les sédiments des estuaires de la Seine et de l'Authie, These de doctorat, Lille 1, 2001.

Birch, G. F.: Determination of sediment metal background concentrations and enrichment in marine environments – A critical review, Science of The Total Environment, 580, 813–831, https://doi.org/10.1016/j.scitotenv.2016.12.028, 2017.

Boguta, P. and Sokołowska, Z.: Zinc Binding to Fulvic acids: Assessing the Impact of pH, Metal Concentrations and Chemical Properties of Fulvic Acids on the Mechanism and Stability of Formed Soluble Complexes, Molecules, 25, 1297, https://doi.org/10.3390/molecules25061297, 2020.

Borůvka, L. and Drábek, O.: Heavy metal distribution between fractions of humic substances in heavily polluted soils, Plant, Soil and Environment, 50, 339–345, https://doi.org/10.17221/4041-PSE, 2004.

Bout-Roumazeilles, V., Cortijo, E., Labeyrie, L., and Debrabant, P.: Clay mineral evidence of nepheloid layer contributions to the Heinrich layers in the northwest Atlantic, Palaeogeography, Palaeoclimatology, Palaeoecology, 146, 211–228, https://doi.org/10.1016/S0031-0182(98)00137-0, 1999.

Bradl, H. B.: Adsorption of heavy metal ions on soils and soils constituents, Journal of Colloid and Interface Science, 277, 1–18, https://doi.org/10.1016/j.jcis.2004.04.005, 2004.

Brady, N. C.: The nature and properties of soils, 9th ed., Macmillan ; Collier Macmillan, New York : London, 750 pp., 1984.

Bronick, C. J. and Lal, R.: Soil structure and management: a review, Geoderma, 124, 3–22, https://doi.org/10.1016/j.geoderma.2004.03.005, 2005.

Cabrera-Real, H., Romero-Serrano, A., Zeifert, B., Hernandez-Ramirez, A., Hallen-Lopez, M., and Cruz-Ramirez, A.: Effect of MgO and CaO/SiO2 on the immobilization of chromium in synthetic slags, Journal of Material Cycles and Waste Management, 14, 317–324, https://doi.org/10.1007/s10163-012-0072-y, 2012.

Calabrese, E. J., Stanek, E. J., James, R. C., and Roberts, S. M.: Soil ingestion: a concern for acute toxicity in children., Environmental Health Perspectives, 105, 1354–1358, https://doi.org/10.1289/ehp.971051354, 1997.

Campillo-Cora, C., Conde-Cid, M., Arias-Estévez, M., Fernández-Calviño, D., and Alonso-Vega, F.: Specific Adsorption of Heavy Metals in Soils: Individual and Competitive Experiments, Agronomy, 10, 1113, https://doi.org/10.3390/agronomy10081113, 2020.

Campos, V.: Trace Elements in Pesticides, Communications in Soil Science and Plant Analysis, 34, 1261–1268, https://doi.org/10.1081/CSS-120020442, 2003.

Casetta, M., Courcot, L., Caillaud, J., Dumoulin, D., Alaimo, V., Cornille, V., Billon, G., Courcot, D., Hermoso, M., and Philippe, S.: Use of potentially toxic elements in sedimentable industrial dust to trace their input in soils (Northern France), J Soils Sediments, 1–21, https://doi.org/10.1007/s11368-024-03817-7, 2024.

Cécillon, L., Baudin, F., Chenu, C., Houot, S., Jolivet, R., Kätterer, T., Lutfalla, S., Macdonald, A., van Oort, F., Plante, A. F., Savignac, F., Soucémarianadin, L. N., and Barré, P.: A model based on Rock-Eval thermal analysis to quantify the size of the centennially persistent organic carbon pool in temperate soils, Biogeosciences, 15, 2835–2849, https://doi.org/10.5194/bg-15-2835-2018, 2018.

Chapman, D. V. (Ed.): Water quality assessments: a guide to the use of biota, sediments and water in environmental monitoring, 2. ed., E & FN Spon, London, 626 pp., 1996.

Chen, C.-W., Kao, C. M., Chen, C.-F., and Dong, C.-D.: Distribution and accumulation of heavy metals in the sediments of Kaohsiung Harbor, Taiwan, Chemosphere, 66, 1431–40, https://doi.org/10.1016/j.chemosphere.2006.09.030, 2007.

Chitolina, G. M., Mendes, K. F., Almeida, C. S., Alonso, F. G., Junqueira, L. V., and Tornisielo, V. L.: Influence of Soil Depth on Sorption and Desorption Processes of Hexazinone, Planta daninha, 38, e020217734, https://doi.org/10.1590/S0100-83582020380100016, 2020.

Crea, F., Foti, C., Milea, D., and Sammartano, S.: Speciation of Cadmium in the Environment, in: Cadmium: From Toxicity to Essentiality, edited by: Sigel, A., Sigel, H., and Sigel, R. K., Springer Netherlands, Dordrecht, 63–83, https://doi.org/10.1007/978-94-007-5179-8_3, 2013.

Crispo, M., Dobson, M. C., Blevins, R. S., Meredith, W., Lake, J. A., and Edmondson, J. L.: Heavy metals and metalloids concentrations across UK urban horticultural soils and the factors influencing their bioavailability to food crops, Environmental Pollution, 288, 117960, https://doi.org/10.1016/j.envpol.2021.117960, 2021.

DesMarais, T. L. and Costa, M.: Mechanisms of Chromium-Induced Toxicity, Curr Opin Toxicol, 14, 1–7, https://doi.org/10.1016/j.cotox.2019.05.003, 2019.

Disnar, J.-R., Guillet, B., Kéravis, D., Di-Giovanni, C., and Sebag, D.: Soil organic matter (SOM) characterization by Rock-Eval pyrolysis :, Organic Geochemistry, 34, 327–343, https://doi.org/10.1016/S0146-6380(02)00239-5, 2003.

Donisa, C., Mocanu, R., and Steinnes, E.: Distribution of some major and minor elements between fulvic and humic acid fractions in natural soils, Geoderma, 111, 75–84, https://doi.org/10.1016/S0016-7061(02)00254-9, 2003.

Douay, F., Pelfrêne, A., Planque, J., Fourrier, H., Richard, A., Roussel, H., and Girondelot, B.: Assessment of potential health risk for inhabitants living near a former lead smelter. Part 1: metal concentrations in soils, agricultural crops, and homegrown vegetables, Environ Monit Assess, 185, 3665–3680, https://doi.org/10.1007/s10661-012-2818-3, 2013.

Dror, I., Yaron, B., and Berkowitz, B.: The Human Impact on All Soil-Forming Factors during the Anthropocene, ACS Environ. Au, 2, 11–19, https://doi.org/10.1021/acsenvironau.1c00010, 2022.

Duchaufour, P.: Humification et écologie, Cahiers ORSTOM.Série Pédologie, 8, 379–390, 1970.

Duchaufour, P., Faivre, P., Poulenard, J., and Gury, M.: Introduction à la science du sol: sol, végétation, environnement : licence 3, master, Capes, Dunod, Malakoff (Hauts-de-Seine), 2020.

Duodu, G. O., Goonetilleke, A., and Ayoko, G. A.: Potential bioavailability assessment, source apportionment and ecological risk of heavy metals in the sediment of Brisbane River estuary, Australia, Mar Pollut Bull, 117, 523–531, https://doi.org/10.1016/j.marpolbul.2017.02.017, 2017.

Duzgoren-Aydin, N. S., Wong, C. S. C., Aydin, A., Song, Z., You, M., and Li, X. D.: Heavy Metal Contamination and Distribution in the Urban Environment of Guangzhou, SE China, Environ Geochem Health, 28, 375–391, https://doi.org/10.1007/s10653-005-9036-7, 2006.

Emadodin, I. and Bork, H. R.: Degradation of soils as a result of long-term human-induced transformation of the environment in Iran: an overview, Journal of Land Use Science, 7, 203–219, https://doi.org/10.1080/1747423X.2011.560292, 2012.

Espitalié, J., Laporte, J. L., Madec, M., Marquis, F., Leplat, P., Paulet, J., and Boutefeu, A.: Méthode rapide de caractérisation des roches mètres, de leur potentiel pétrolier et de leur degré d’évolution, Rev. Inst. Fr. Pét., 32, 23–42, https://doi.org/10.2516/ogst:1977002, 1977.

Espitalié, J., Deroo, G., and Marquis, F.: La pyrolyse Rock-Eval et ses applications. Deuxième partie., Rev. Inst. Fr. Pét., 40, 755–784, https://doi.org/10.2516/ogst:1985045, 1985.

Falsone, G., Celi, L., Caimi, A., Simonov, G., and Bonifacio, E.: The effect of clear cutting on podzolisation and soil carbon dynamics in boreal forests (Middle Taiga zone, Russia), Geoderma, 177–178, 27–38, https://doi.org/10.1016/j.geoderma.2012.01.036, 2012.

FAO (Ed.): World reference base for soil resources 2014: international soil classification system for naming soils and creating legends for soil maps, FAO, Rome, 2014.

FAO and UNEP: Global assessment of soil pollution - Summary for policy makers, Rome, FAO, https://doi.org/10.4060/cb4827en, 2021.

Feng, X., Hong, Y., Hong, B., and Ni, J.: Mobility of some potentially toxic trace elements in the coal of Guizhou, China, Environmental Geology, 39, 372–377, https://doi.org/10.1007/s002540050016, 2000.

Fernández-Turiel, J. L., de Carvalho, W., Cabañas, M., Querol, X., and López-Soler, A.: Mobility of heavy metals from coal fly ash, Geo, 23, 264–270, https://doi.org/10.1007/BF00766741, 1994.

Fiedler, S., Vepraskas, M. J., and Richardson, J. L.: Soil Redox Potential: Importance, Field Measurements, and Observations, in: Advances in Agronomy, vol. 94, edited by: Sparks, D. L., Academic Press, 1–54, https://doi.org/10.1016/S0065-2113(06)94001-2, 2007.

Fijałkowski, K., Kacprzak, M., Grobelak, A., and Placek, A.: The influence of selected soil parameters on the mobility of heavy metals in soil, Inżynieria i Ochrona Środowiska/Engineering and Protection of Environment, 15, 81–92, 2012.

Gardner, M., Comber, S., Scrimshaw, M. D., Cartmell, E., Lester, J., and Ellor, B.: The significance of hazardous chemicals in wastewater treatment works effluents, Science of The Total Environment, 437, 363–372, https://doi.org/10.1016/j.scitotenv.2012.07.086, 2012.

Pollution des sols, SIS et anciens sites industriels: https://www.georisques.gouv.fr/risques/sites-et-sols-pollues/donnees, last access: 17 April 2023.

Registre des émissions polluantes: https://www.georisques.gouv.fr/risques/registre-des-emissions-polluantes/etablissement/donnees, last access: 17 April 2023.

Girard, M.-C.: Sols et environnement : cours, exercices et études de cas, Dunod, Paris, 2005.

GIS Sol and RMT Sols et Territoires: Pédologie – Les sols dominants de France métropolitaine, 2019.

Goix, S., Mombo, S., Schreck, E., Pierart, A., Lévêque, T., Deola, F., and Dumat, C.: Field isotopic study of lead fate and compartmentalization in earthworm–soil–metal particle systems for highly polluted soil near Pb recycling factory, Chemosphere, 138, 10–17, https://doi.org/10.1016/j.chemosphere.2015.05.010, 2015.

Goldberg, S., Forster, H. s., and Godfrey, C. l.: Molybdenum Adsorption on Oxides, Clay Minerals, and Soils, Soil Science Society of America Journal, 60, 425–432, https://doi.org/10.2136/sssaj1996.03615995006000020013x, 1996.

Guo, G., Wu, F., Xie, F., and Zhang, R.: Spatial distribution and pollution assessment of heavy metals in urban soils from southwest China, Journal of Environmental Sciences, 24, 410–418, https://doi.org/10.1016/S1001-0742(11)60762-6, 2012.

Hailegnaw, N. S., Bayabil, H. K., Li, Y. C., and Gao, B.: Seawater flooding of calcareous soils: Implications for trace and alkaline metals mobility, Science of The Total Environment, 927, 172210, https://doi.org/10.1016/j.scitotenv.2024.172210, 2024.

Hamdoun, H., Leleyter, L., Van-Veen, E., Coggan, J., Basset, B., Lemoine, M., and Baraud, F.: Comparison of three procedures (single, sequential and kinetic extractions) for mobility assessment of Cu, Pb and Zn in harbour sediments, Comptes Rendus Geoscience, 347, 94–102, https://doi.org/10.1016/j.crte.2015.03.003, 2015.

Han, L., Chen, B., Liu, T., and Choi, Y.: Leaching Characteristics of Iron and Manganese from Steel Slag with Repetitive Replenishment of Leachate, KSCE J Civ Eng, 23, 3297–3304, https://doi.org/10.1007/s12205-019-0250-8, 2019.

Hanna, K., Lassabatere, L., and Bechet, B.: Zinc and lead transfer in a contaminated roadside soil: Experimental study and modeling, Journal of Hazardous Materials, 161, 1499–1505, https://doi.org/10.1016/j.jhazmat.2008.04.124, 2009.

Harb, M. K., Ebqa’ai, M., Al-rashidi, A., Alaziqi, B. H., Al Rashdi, M. S., and Ibrahim, B.: Investigation of selected heavy metals in street and house dust from Al-Qunfudah, Kingdom of Saudi Arabia, Environmental earth sciences, 2015.

He, Z. L., Yang, X. E., and Stoffella, P. J.: Trace elements in agroecosystems and impacts on the environment, Journal of Trace Elements in Medicine and Biology, 19, 125–140, https://doi.org/10.1016/j.jtemb.2005.02.010, 2005.

Hernandez-Soriano, M. C. and Jimenez-Lopez, J. C.: Effects of soil water content and organic matter addition on the speciation and bioavailability of heavy metals, Science of The Total Environment, 423, 55–61, https://doi.org/10.1016/j.scitotenv.2012.02.033, 2012.

Hetényi, M. and Nyilas, T.: Soil Organic Matter Characterization Using S3 and S4 Signals from Rock-Eval Pyrolysis, Pedosphere, 24, 563–574, https://doi.org/10.1016/S1002-0160(14)60042-4, 2014.

Hleis, D., Fernández-Olmo, I., Ledoux, F., Kfoury, A., Courcot, L., Desmonts, T., and Courcot, D.: Chemical profile identification of fugitive and confined particle emissions from an integrated iron and steelmaking plant, Journal of Hazardous Materials, 250–251, 246–255, https://doi.org/10.1016/j.jhazmat.2013.01.080, 2013.

Holtzapffel, T.: Les minéraux argileux: préparation, analyse diffractométrique et détermination, Société géologique du Nord, 1985.

Impellitteri, C. A., Lu, Y., Saxe, J. K., Allen, H. E., and Peijnenburg, W. J. G. M.: Correlation of the partitioning of dissolved organic matter fractions with the desorption of Cd, Cu, Ni, Pb and Zn from 18 Dutch soils, Environment International, 28, 401–410, https://doi.org/10.1016/S0160-4120(02)00065-X, 2002.

Kandpal, G., Srivastava, P. C., and Ram, B.: Kinetics of Desorption of Heavy Metals from Polluted Soils: Influence of Soil Type and Metal Source, Water Air Soil Pollut, 161, 353–363, https://doi.org/10.1007/s11270-005-5548-0, 2005.

Kassambara, A. and Mundt, F.: Extract and Visualize the Results of Multivariate Data Analyses [R package factoextra version 1.0.7], 2020.

Kfoury, A., Ledoux, F., Roche, C., Delmaire, G., Roussel, G., and Courcot, D.: PM2.5 source apportionment in a French urban coastal site under steelworks emission influences using constrained non-negative matrix factorization receptor model, Journal of Environmental Sciences, 40, 114–128, https://doi.org/10.1016/j.jes.2015.10.025, 2016.

Khademi, H., Gabarrón, M., Abbaspour, A., Martínez-Martínez, S., Faz, A., and Acosta, J. A.: Environmental impact assessment of industrial activities on heavy metals distribution in street dust and soil, Chemosphere, 217, 695–705, https://doi.org/10.1016/j.chemosphere.2018.11.045, 2019.

Kicińska, A.: Physical and chemical characteristics of slag produced during Pb refining and the environmental risk associated with the storage of slag, Environ Geochem Health, 43, 2723–2741, https://doi.org/10.1007/s10653-020-00738-5, 2021.

Kubier, A., Wilkin, R. T., and Pichler, T.: Cadmium in soils and groundwater: A review, Appl Geochem, 108, 1–16, https://doi.org/10.1016/j.apgeochem.2019.104388, 2019.

Kubová, J., Matúš, P., Bujdoš, M., Hagarová, I., and Medveď, J.: Utilization of optimized BCR three-step sequential and dilute HCl single extraction procedures for soil–plant metal transfer predictions in contaminated lands, Talanta, 75, 1110–1122, https://doi.org/10.1016/j.talanta.2008.01.002, 2008.

Lafargue, E., Marquis, F., and Pillot, D.: Rock-Eval 6 Applications in Hydrocarbon Exploration, Production, and Soil Contamination Studies, Rev. Inst. Fr. Pét., 53, 421–437, https://doi.org/10.2516/ogst:1998036, 1998.

Lasota, J., Błońska, E., Łyszczarz, S., and Tibbett, M.: Forest Humus Type Governs Heavy Metal Accumulation in Specific Organic Matter Fractions, Water Air Soil Pollut, 231, 80, https://doi.org/10.1007/s11270-020-4450-0, 2020.

Lê, S., Josse, J., and Husson, F.: FactoMineR : A Package for Multivariate Analysis, J. Stat. Soft., 25, https://doi.org/10.18637/jss.v025.i01, 2008.

Lee, C. S., Li, X., Shi, W., Cheung, S. C., and Thornton, I.: Metal contamination in urban, suburban, and country park soils of Hong Kong: A study based on GIS and multivariate statistics, Science of The Total Environment, 356, 45–61, https://doi.org/10.1016/j.scitotenv.2005.03.024, 2006.

Leifeld, J. and Kögel-Knabner, I.: Organic carbon and nitrogen in fine soil fractions after treatment with hydrogen peroxide, Soil Biology and Biochemistry, 33, 2155–2158, https://doi.org/10.1016/S0038-0717(01)00127-4, 2001.

Leplat, J., Sommé, J., Baeteman, C., and Paepe, R.: Carte géologique de la France à 1/50 000 - DUNKERQUE-HONDSCHOOTE, 1988.

Li, X., Lan, X., Liu, W., Cui, X., and Cui, Z.: Toxicity, migration and transformation characteristics of lead in soil-plant system: Effect of lead species, Journal of Hazardous Materials, 395, 122676, https://doi.org/10.1016/j.jhazmat.2020.122676, 2020.

Li, Z. and Shuman, L. M.: Heavy metal movement in metal-contaminated soil profiles, Soil Science, 161, https://doi.org/10.1097/00010694-199610000-00003, 1996.

Luo, W. T., Nelson, P. N., Li, M.-H., Cai, J. P., Zhang, Y. Y., Zhang, Y. G., Yang, S., Wang, R. Z., Wang, Z. W., Wu, Y. N., Han, X. G., and Jiang, Y.: Contrasting pH buffering patterns in neutral-alkaline soils along a 3600 km transect in northern China, Biogeosciences, 12, 7047–7056, https://doi.org/10.5194/bg-12-7047-2015, 2015.

Madrid, F., Reinoso, R., Florido, M. C., Díaz Barrientos, E., Ajmone-Marsan, F., Davidson, C. M., and Madrid, L.: Estimating the extractability of potentially toxic metals in urban soils: A comparison of several extracting solutions, Environmental Pollution, 147, 713–722, https://doi.org/10.1016/j.envpol.2006.09.005, 2007.

Manta, D. S., Angelone, M., Bellanca, A., Neri, R., and Sprovieri, M.: Heavy metals in urban soils: a case study from the city of Palermo (Sicily), Italy, Science of The Total Environment, 300, 229–243, https://doi.org/10.1016/S0048-9697(02)00273-5, 2002.

Minami, K.: Soil and humanity: Culture, civilization, livelihood and health, Soil Science and Plant Nutrition, 55, 603–615, https://doi.org/10.1111/j.1747-0765.2009.00401.x, 2009.

Mombelli, D., Mapelli, C., Barella, S., Di Cecca, C., Le Saout, G., and Garcia-Diaz, E.: The effect of microstructure on the leaching behaviour of electric arc furnace (EAF) carbon steel slag, Process Safety and Environmental Protection, 102, 810–821, https://doi.org/10.1016/j.psep.2016.05.027, 2016.

Ortega Montoya, C. Y., López-Pérez, A. O., Ugalde Monzalvo, M., and Ruvalcaba Sánchez, Ma. L. G.: Multidimensional Urban Exposure Analysis of Industrial Chemical Risk Scenarios in Mexican Metropolitan Areas, Int J Environ Res Public Health, 18, 5674, https://doi.org/10.3390/ijerph18115674, 2021.

Orucoglu, E., Grangeon, S., Gloter, A., Robinet, J.-C., Madé, B., and Tournassat, C.: Competitive Adsorption Processes at Clay Mineral Surfaces: A Coupled Experimental and Modeling Approach, ACS Earth Space Chem., 6, 144–159, https://doi.org/10.1021/acsearthspacechem.1c00323, 2022.

Otunola, B. O. and Ololade, O. O.: A review on the application of clay minerals as heavy metal adsorbents for remediation purposes, Environmental Technology & Innovation, 18, 100692, https://doi.org/10.1016/j.eti.2020.100692, 2020.

Palansooriya, K. N., Shaheen, S. M., Chen, S. S., Tsang, D. C. W., Hashimoto, Y., Hou, D., Bolan, N. S., Rinklebe, J., and Ok, Y. S.: Soil amendments for immobilization of potentially toxic elements in contaminated soils: A critical review, Environment International, 134, 105046, https://doi.org/10.1016/j.envint.2019.105046, 2020.

Panagos, P., Ballabio, C., Lugato, E., Jones, A., Borrelli, P., Scarpa, S., Orgiazzi, A., and Montanarella, L.: Potential Sources of Anthropogenic Copper Inputs to European Agricultural Soils, Sustainability, 10, 2380, https://doi.org/10.3390/su10072380, 2018.

Pelfrêne, A., Sahmer, K., Waterlot, C., Glorennec, P., Douay, F., and Le Bot, B.: Evaluation of single-extraction methods to estimate the oral bioaccessibility of metal(loid)s in soils, Science of The Total Environment, 727, 138553, https://doi.org/10.1016/j.scitotenv.2020.138553, 2020.

Pellegrini, E., Contin, M., Mazhar, S., Bravo, C., and De Nobili, M.: Flooding by sea and brackish waters enhances mobility of Cd, Zn and Pb from airborne dusts in coastal soils, Science of The Total Environment, 922, 171038, https://doi.org/10.1016/j.scitotenv.2024.171038, 2024.

Philippe, S., Leterme, C., Lesourd, S., Courcot, L., Haack, U., and Caillaud, J.: Bioavailability of sediment-borne lead for ragworms (Hediste diversicolor) investigated by lead isotopes, Applied Geochemistry, 23, 2932–2944, https://doi.org/10.1016/j.apgeochem.2008.04.012, 2008.

Preston, C. M. and Schmidt, M. W. I.: Black (pyrogenic) carbon: a synthesis of current knowledge and uncertainties with special consideration of boreal regions, Biogeosciences, 3, 397–420, https://doi.org/10.5194/bg-3-397-2006, 2006.

QGIS Development Team: QGIS Geographic Information System. Open Source Geospatial Foundation Project, 2023.

Querol, X., Fernández-Turiel, J., and López-Soler, A.: Trace elements in coal and their behaviour during combustion in a large power station, Fuel, 74, 331–343, https://doi.org/10.1016/0016-2361(95)93464-O, 1995.

R Core Team: R: A Language and Environment for Statistical Computing, 2022.

Rajmohan, N., Prathapar, S. A., Jayaprakash, M., and Nagarajan, R.: Vertical distribution of heavy metals in soil profile in a seasonally waterlogging agriculture field in Eastern Ganges Basin, Environ Monit Assess, 186, 5411–5427, https://doi.org/10.1007/s10661-014-3790-x, 2014.

Rao, C. R. M., Sahuquillo, A., and Lopez-Sanchez, J. F.: Comparison of single and sequential extraction procedures for the study of rare earth elements remobilisation in different types of soils, Analytica Chimica Acta, 662, 128–136, https://doi.org/10.1016/j.aca.2010.01.006, 2010.

Reimann, C. and De Caritat, P.: Chemical elements in the environment: factsheets for the geochemist and environmental scientist, Springer, Berlin ; New York, 397 pp., 1998.

Ren, Z. L., Sivry, Y., Dai, J., Tharaud, M., Cordier, L., and Benedetti, M. F.: Multi-element stable isotopic dilution and multi-surface modelling to assess the speciation and reactivity of cadmium and copper in soil, European Journal of Soil Science, 66, 973–982, https://doi.org/10.1111/ejss.12298, 2015.

Rengasamy, P. and Churchman, G. J.: Cation exchange capacity, exchangeable cations and sodicity, Collingwood, Vic, CSIRO Publishing, 1999.

Richer-De-Forges, A. C., Feller, C., Jamagne, M., and Arrouays, D. D.: Perdus dans le triangle des textures, Etude et Gestion des Sols, 15, 97, 2008.

Roosa, S., Prygiel, E., Lesven, L., Wattiez, R., Gillan, D., Ferrari, B. J. D., Criquet, J., and Billon, G.: On the bioavailability of trace metals in surface sediments: a combined geochemical and biological approach, Environ Sci Pollut Res, 23, 10679–10692, https://doi.org/10.1007/s11356-016-6198-z, 2016.

Saenger, A., Cécillon, L., Sebag, D., and Brun, J.-J.: Soil organic carbon quantity, chemistry and thermal stability in a mountainous landscape: A Rock–Eval pyrolysis survey, Organic Geochemistry, 54, 101–114, https://doi.org/10.1016/j.orggeochem.2012.10.008, 2013.

dos Santos, J. V., Fregolente, L. G., Mounier, S., Hajjoul, H., Ferreira, O. P., Moreira, A. B., and Bisinoti, M. C.: Fulvic acids from Amazonian anthropogenic soils: Insight into the molecular composition and copper binding properties using fluorescence techniques, Ecotoxicology and Environmental Safety, 205, 111173, https://doi.org/10.1016/j.ecoenv.2020.111173, 2020.

Sarkar, B., Mukhopadhyay, R., Ramanayaka, S., Bolan, N., and Ok, Y. S.: The role of soils in the disposition, sequestration and decontamination of environmental contaminants, Philosophical Transactions of the Royal Society B: Biological Sciences, 376, 20200177, https://doi.org/10.1098/rstb.2020.0177, 2021.

Schnitzer, M. and Kerndorff, H.: Reactions of fulvic acid with metal ions, Water Air Soil Pollut, 15, 97–108, https://doi.org/10.1007/BF00285536, 1981.

Schulin, R., Curchod, F., Mondeshka, M., Daskalova, A., and Keller, A.: Heavy metal contamination along a soil transect in the vicinity of the iron smelter of Kremikovtzi (Bulgaria), Geoderma, 140, 52–61, https://doi.org/10.1016/j.geoderma.2007.03.007, 2007.

Smedley, P. L. and Kinniburgh, D. G.: Molybdenum in natural waters: A review of occurrence, distributions and controls, Applied Geochemistry, 84, 387–432, https://doi.org/10.1016/j.apgeochem.2017.05.008, 2017.

Smith, P., Cotrufo, M. F., Rumpel, C., Paustian, K., Kuikman, P. J., Elliott, J. A., McDowell, R., Griffiths, R. I., Asakawa, S., Bustamante, M., House, J. I., Sobocká, J., Harper, R., Pan, G., West, P. C., Gerber, J. S., Clark, J. M., Adhya, T., Scholes, R. J., and Scholes, M. C.: Biogeochemical cycles and biodiversity as key drivers of ecosystem services provided by soils, SOIL, 1, 665–685, https://doi.org/10.5194/soil-1-665-2015, 2015.

Smolders, E. and Degryse, F.: Fate and Effect of Zinc from Tire Debris in Soil, Environ. Sci. Technol., 36, 3706–3710, https://doi.org/10.1021/es025567p, 2002.

Snape, I., Scouller, R. C., Stark, S. C., Stark, J., Riddle, M. J., and Gore, D. B.: Characterisation of the dilute HCl extraction method for the identification of metal contamination in Antarctic marine sediments, Chemosphere, 57, 491–504, https://doi.org/10.1016/j.chemosphere.2004.05.042, 2004.

Soil Science Division Staff: Soil survey manual. C. Ditzler, K. Scheffe, and H.C. Monger (eds.). USDA Handbook 18. Government Printing Office, Washington, D.C., 639, 2017.

Stavi, I., Bel, G., and Zaady, E.: Soil functions and ecosystem services in conventional, conservation, and integrated agricultural systems. A review, Agron. Sustain. Dev., 36, 32, https://doi.org/10.1007/s13593-016-0368-8, 2016.

Sterckeman, T., Douay, F., Proix, N., and Fourrier, H.: Vertical distribution of Cd, Pb and Zn in soils near smelters in the North of France, Environmental Pollution, 107, 377–389, https://doi.org/10.1016/S0269-7491(99)00165-7, 2000.

Sterckeman, T., Douay, F., Baize, D., Fourrier, H., Proix, N., and Schvartz, C.: Factors affecting trace element concentrations in soils developed on recent marine deposits from northern France, Applied Geochemistry, 19, 89–103, https://doi.org/10.1016/S0883-2927(03)00085-4, 2004.

Sun, J., Yu, R., Hu, G., Su, G., and Zhang, Y.: Tracing of heavy metal sources and mobility in a soil depth profile via isotopic variation of Pb and Sr, CATENA, 171, 440–449, https://doi.org/10.1016/j.catena.2018.07.040, 2018.

Taylor, S. R. and McLennan, S. M.: The geochemical evolution of the continental crust, Reviews of Geophysics, 33, 241–265, https://doi.org/10.1029/95RG00262, 1995.

Tetteh, R. N.: Chemical soil degradation as a result of contamination: A review, JSSEM, 6, 301–308, https://doi.org/10.5897/JSSEM15, 2015.

Townsend, A. T., Palmer, A. S., Stark, S. C., Samson, C., Scouller, R. C., and Snape, I.: Trace metal characterisation of marine sediment reference materials MESS-3 and PACS-2 in dilute HCl extracts, Marine Pollution Bulletin, 54, 236–239, https://doi.org/10.1016/j.marpolbul.2006.11.002, 2007.

Vandenbroucke, M. and Largeau, C.: Kerogen origin, evolution and structure, Organic Geochemistry, 38, 719–833, https://doi.org/10.1016/j.orggeochem.2007.01.001, 2007.

Varadachari, C., Mondal, A. H., Dulal C., N., and Ghosh, K.: Clay-humus complexation: Effect of pH and the nature of bonding, Soil Biology and Biochemistry, 26, 1145–1149, https://doi.org/10.1016/0038-0717(94)90136-8, 1994.

Warwick, P., Hall, A., Pashley, V., Van der Lee, J., and Maes, A.: Zinc and cadmium mobility in sand: effects of pH, speciation, Cation Exchange Capacity (CEC), humic acid and metal ions, Chemosphere, 36, 2283–2290, https://doi.org/10.1016/S0045-6535(97)10197-7, 1998.

Waterlot, C., Douay, F., and Pelfrêne, A.: Chemical Availability of Cd, Pb and Zn in Anthropogenically Polluted Soil: Assessing the Geochemical Reactivity and Oral Bioaccessibility, Pedosphere, 27, 616–629, https://doi.org/10.1016/S1002-0160(17)60356-4, 2017.

Wei, T. and Simko, V.: R package “corrplot”: Visualization of a Correlation Matrix, 2021.

Wickham, H.: ggplot2: Elegant Graphics for Data Analysis, 2nd ed. 2016., Springer International Publishing : Imprint: Springer, Cham, 1 pp., https://doi.org/10.1007/978-3-319-24277-4, 2016.

Williams, D. E., Vlamis, J., Pukite, A. H., and Corey, J. E.: METAL MOVEMENT IN SLUDGE-AMENDED SOILS: A NINE-YEAR STUDY, Soil Science, 143, 124, 1987.

Ye, C., Li, S., Zhang, Y., and Zhang, Q.: Assessing soil heavy metal pollution in the water-level-fluctuation zone of the Three Gorges Reservoir, China, J Hazard Mater, 191, 366–372, https://doi.org/10.1016/j.jhazmat.2011.04.090, 2011.

Yong, R. N., Mohamed, A.-M. O., and Warkentin, B. P.: Principles of contaminant transport in soils, Elsevier, Amsterdam ; New York, 327 pp., 1992.

Yu, D., Qiu, W., Zhang, Z., Glass, K., Su, J., DeMeo, D. L., Tantisira, K., and Weiss, S. T.: corTest: Robust Tests for Equal Correlation, 2020.

Yu, H., Li, C., Yan, J., Ma, Y., Zhou, X., Yu, W., Kan, H., Meng, Q., Xie, R., and Dong, P.: A review on adsorption characteristics and influencing mechanism of heavy metals in farmland soil, RSC Adv., 13, 3505–3519, https://doi.org/10.1039/D2RA07095B, 2023.

Yu, Z., Liu, E., Lin, Q., Zhang, E., Yang, F., Wei, C., and Shen, J.: Comprehensive assessment of heavy metal pollution and ecological risk in lake sediment by combining total concentration and chemical partitioning, Environmental Pollution, 269, 116212, https://doi.org/10.1016/j.envpol.2020.116212, 2021.

Zhao, S., Duan, Y., Lu, J., Gupta, R., Pudasainee, D., Liu, S., Liu, M., and Lu, J.: Chemical speciation and leaching characteristics of hazardous trace elements in coal and fly ash from coal-fired power plants, Fuel, 232, 463–469, https://doi.org/10.1016/j.fuel.2018.05.135, 2018.

Zhuang, P., McBride, M. B., Xia, H., Li, N., and Li, Z.: Health risk from heavy metals via consumption of food crops in the vicinity of Dabaoshan mine, South China, Science of The Total Environment, 407, 1551–1561, https://doi.org/10.1016/j.scitotenv.2008.10.061, 2009.